Biogeosciences Discuss., doi:10.5194/bg-2017-114, 2017
Manuscript under review for journal Biogeosciences
Discussion started: 28 April 2017

Optimization of Biological Production for Indian Ocean upwelling zones: Part – I: Improving Biological Parameterization via a variable Compensation Depth

Mohanan Geethalekshmi Sreeush[1,2,*].

Vinu Valsala[1],

Sreenivas Pentakota[1],

Koneru Venkata Siva Rama Prasad[2],

Raghu Murtugudde[3]

[1]Indian Institute of Tropical Meteorology, Pune, India

[2]Department of Meteorology and Physical Oceanography, Andhra University, India

[3]ESSIC, University of Maryland, USA

*Corresponding author address:
Indian Institute of Tropical Meteorology,
Dr. Homibhabha Road, Pashan, Pune 411 008, India
E-Mail: sreeushmg@tropmet.res.in

Biogeosciences Discuss., doi:10.5194/bg-2017-114, 2017
Manuscript under review for journal Biogeosciences
Discussion started: 28 April 2017

Abstract

Biological modeling approach adopted by the Ocean Carbon Cycle Model Inter-comparison Project (OCMIP-II) provided amazingly simple but surprisingly accurate rendition of the annual mean carbon cycle for the global ocean. Nonetheless, OCMIP models are known to have seasonal biases which are typically attributed to their bulk parameterization of 'compensation depth'. Utilizing the principle of minimum solar radiation for the production and its attenuation by the surface Chl-a, we have proposed a new parameterization for a spatially and temporally varying 'compensation depth' which captures the seasonality in the production zone reasonably well. This new parameterization is shown to improve the seasonality of CO_2 fluxes, surface ocean pCO_2, biological export and new production in the major upwelling zones of the Indian Ocean. The seasonally varying compensation depth enriches the nutrient concentration in the upper ocean yielding more faithful biological exports which in turn leads to an accurate seasonality in carbon cycle. The export production strengthens by ~70% over western Arabian sea during monsoon period and achieved a good balance between export and new production in the model. This underscores the importance of having a seasonal balance in model export and new production for a better representation of the seasonality of carbon cycle over upwelling regions The study also implies that both the biological and solubility pumps play an important role in the Indian Ocean upwelling zones.

Keywords: Indian Ocean upwelling zones, Carbon cycle, Seasonal cycle - CO_2 flux and Oceanic pCO_2, Biogeochemical model parameterization, Export production - New production balance.

Biogeosciences Discuss., doi:10.5194/bg-2017-114, 2017
Manuscript under review for journal Biogeosciences
Discussion started: 28 April 2017

1. Introduction

Among the world's oceans, Indian Ocean is characterized by a unique seasonally reversing wind systems called monsoon winds. The monsoon winds are the major physical drivers for the coastal and open ocean upwelling in the Indian Ocean. The major upwelling systems in the Indian Ocean are (1) the western Arabian Sea (WAS; Ryther et. al., 1965, Smith et. al., 2001, Sarma., 2004, Wiggert et. al., 2006, Murtugudde et. al., 2007, McCreary et. al., 2009, Prasanna Kumar et. al., 2010, Naqvi et. al., 2010, Roxy et al., 2015) (2) the SriLanka Dome (SLD;Vinayachandran et al., 1998, 2004), (3) Java and Sumatra coasts (SC; Murtugudde et al., 1999, Susanto et. al., 2001, Osawa et. al., 2010, Xing et. al., 2012) and (4) the Seychelles-Chagos thermocline ridge (SCTR; Dilmahamod., 2016, Figure 1). The physical and biological processes and their variability over these key regions are inseparably tied to the strength of the monsoon winds and associated nutrient dynamics. The production and variability in the coastal upwelling systems are a key concern to the fishing community, since they affect the day-to-day livelihood of the coastal populations (Harvell et. al., 1999, Roxy et. al., 2015, Praveen et al., 2016). Coastal upwelling systems account for about 11% of the world oceanic biological production (Prasanna Kumar et al., 2001, Wiggert et al., 2005, Levy et al., 2007, McCreary et al., 2009, Liao et. al., 2016) and are especially important for the Indian Ocean rim countries due to their developing countries status.

Arabian Sea is a highly productive coastal upwelling system characterized by phytoplankton blooms both in summer (Prasanna Kumar et al., 2001, Naqvi et al., 2003, Wiggert et al., 2005) and winter (Banse K. et. al., 1986, Schubert et. al., 1998, Wiggert et. al., 2000, Barber et. al., 2001, Prasannakumar et al., 2001, Sarma., 2004). Arabian Sea is known for the second largest Tuna fishing region among all oceans (Lee et al., 2005). The Somali and Omani upwelling

Biogeosciences Discuss., doi:10.5194/bg-2017-114, 2017
Manuscript under review for journal Biogeosciences
Discussion started: 28 April 2017

regions experience phytoplankton blooms that are prominent with Net Primary Production (NPP) exceeding 438.29 g C m^{-2} yr^{-1} (Liao et. al., 2016). On the other hand productivity over the SLD (Vinayachandran and Yamagata, 1998), in the sea of Sri Lanka is triggered by an open ocean Ekman suction. SLD shows strong Chl-a blooms during the summer monsoon (Murtugudde et al., 1999, Vinayachandran et al., 2004). Compared to the Arabian Sea this bloom lasts for more than four months due to the impact of biogeochemistry of the region (Vinayachandran et. al., 2004). During the winter monsoon, the southwest Bay of Bengal is also characterized by Chl-a blooms associated with the intense cyclonic activities (Vinayachandran and Mathew, 2003).

The SC upwelling is basically due to the stronger alongshore winds and its variation is associated with impact of equatorial and coastal Kelvin waves (Murtugudde et. al., 2000). The interannual variability associated with Java-Sumatra coastal upwelling is strongly coupled with ENSO (El-Nino Southern Oscillation) through Indonesian throughflow (Susanto. et. al., 2001, Valsala et al., 2011) and peaks in July through August with a potential new production of 1.02 x 10^{14} g C yr^{-1} (Xing et. al., 2012).

The SCTR region productivity has large spatial and interannual variability. The warmer upper ocean condition associated with El Nino reduce the amplitude of the subseasonal SST variability over the SCTR (Jung and Kirtman., 2016). The Chl-a concentration peaks in summer when the southeast trade winds induce mixing and initiate the upwelling of nutrient-rich water (Murtugudde et. al., 1999, Wiggert et al., 2006, Vialard. J. et. al., 2009, Dilmahamod et al., 2016).

Understanding the biological production and variability in the upwelling systems are important because it gives us crucial information regarding marine species variability (Colwell,

Biogeosciences Discuss., doi:10.5194/bg-2017-114, 2017
Manuscript under review for journal Biogeosciences
Discussion started: 28 April 2017

1996, Harvell et al., 1999, Selina et al., 2015). The observations also provide vital insights into physical and biological interactions of the ecosystem (Naqvi et al., 2010) although limitations of sparse observations often force us to depend on models to examine the large spatio-temporal variability of the ecosystem (Valsala et al., 2013). Simple to inter-mediate complex marine ecosystem models have been employed by several of the previous studies (Sarmiento et. al., 2000, Orr. et. al., 2001, Matsumoto et. al., 2008). However the representation of marine ecosystem variability by proper parameterizations in models has always been a daunting task. This is impediment to the accurate representation of biological primary and export productions in models (Friedrichs et al., 2006, 2007) and the parameterization issues also impact the modeling of upper trophics levels (Lehodey et al., 2010).

Biological production can be quantified with a better understanding of primary production by phytoplankton. Primary production depends on water temperature, light and nutrient availability (Brock. et. al., 1993, Moisan et. al., 2002) and this became the key reason for parameterizing the production in models as one or more combinations of these terms (Yamanaka et. al., 2004). Any of these parameters can be tweaked to alter production in models. For example the availability of nutrients and light determines the phytoplankton growth (Eppely et al., 1972) or growth rate (Boyd et. al., 2013). Stoichiometry and carbon-to-Chl-a ratios are other important factors to be considered in modeling (Christian et al., 2001, Wang et al., 2009) but we will not consider them in this study.

In 1995, an initiative by the IGBP/GAIM (International Geosphere-Biosphere program/Global Analysis, Integration and Modeling) and IGBP/JGOFS (Joint Global Ocean Flux Study) to study carbon cycle referred to as the Ocean Carbon cycle Model Intercomparison Project (OCMIP) greatly improved our understanding of global carbon cycle (Raymond Najjar

Biogeosciences Discuss., doi:10.5194/bg-2017-114, 2017
Manuscript under review for journal Biogeosciences
Discussion started: 28 April 2017

and James Orr, 1998). OCMIP-II further introduced a simple phosphate dependent production term in biological models for long term simulations of carbon cycle (Najjar et al, 1998). Although OCMIP – II is a very simplified model, it is surprisingly accurate in simulating the annual mean state and the response to anthropogenic climate change (Orr et al., 2001, Doney et. al., 2004). However, the OCMIP – II model simulations comes with a penalty of higher seasonal biases when compared with observations (Orr et al., 2003). In this protocol the light limitation is formulated as a bulk quantity with the notion that the minimum light irradiance at which phytoplankton photosynthesis is sufficient to balance the community respiration, Ic, is the compensation irradiance (Sarmiento et al., 2006) and the depth at which the photosynthesis equals respiration is the compensation depth Zc (Smetacek and Passow, 1990), which is clearly different from the conventional euphotic zone depth (Morel., 1988). If the irradiance is below Ic, phytoplankton growth will be suppressed. If the irradiance is above this, the planktonic photosynthesis will exceed the community respiration and production will increase (Parsons et. al., 1984, Sarmiento et. al., 2006). Therefore the compensation depth represents the oceanic production zone in this approach.

However, Zc was held constant in time and space in OCMIP-II models (Raymond Najjar and James Orr, 1998, Matsumoto et. al., 2008) though in reality Zc varies in space and time (Najjar and Keeling, 1997) just as the euphotic zone depth does as documented in ship measurements (Qasim, 1977, 1982). The variation in compensation depth indicates the seasonality of the production zone itself. Availability of light and nutrients at an optimum level is clearly essential for primary production.

Most of the biophysical models prescribe a constant value for compensation depth (e.g., Zc = 75m in OCMIP –II protocol (Raymond Najjar and James Orr, 1998), Zc = 100m for Minnestoa

Biogeosciences Discuss., doi:10.5194/bg-2017-114, 2017
Manuscript under review for journal Biogeosciences
Discussion started: 28 April 2017

Earth System Model (Matsumoto et. al., 2008) although in reality it is not a constant. Depending on the latitude, compensation depth varies between 50m and 100m in the real world (Najjar and Keeling, 1997). In our study we have attempted a novel biological parameterization scheme for spatially and temporally varying compensation depth in the OCMIP – II framework by representing it as a function of optimum solar radiation (Parsons et. al., 1984) and Chl-a availability. In this hypothesis, the minimum solar radiation required for photosynthesis is taken as 10 W m^{-2} below which the production reduces to 20% (Parsons et. al., 1984) and the Chl-a concentration which determines the attenuation of solar radiation with depth in the production zone is also assumed to vary to yield the spatio-temporal variability of Zc. The basic currency of phosphate will act as limiting factor for biological production within this varying compensation depth. This spatially and temporally varying compensation depth represents the seasonality in the production zone.

Regions of sustained upwelling like the eastern equatorial Pacific are well understood in terms of the role of upwelling in increasing the surface water pCO_2 to drive an outgassing of CO_2 into the atmosphere (Feely et al., 1999, Valsala et al., 2014). The Indian Ocean on the other hand only experiences seasonal upwelling which is relatively weak in the deep tropics but stronger off the coasts of Somalia and Oman and in the SLD region (Valsala et al., 2013). The relative importance of the solubility vs. biological pump is not well understood. Our focus here on implementing seasonality in the compensation depth of OCMIP models nonetheless leads to new insights on the impact of improved biological production on surface water pCO_2 and air-sea CO_2 fluxes. The largely positive effects of the variable compensation depth over the Indian Ocean and the sensitivity experiments where upwelling is muted strongly imply that the biological pump may play as much of role as the solubility pump in determining surface pCO_2 and CO_2 fluxes.

Biogeosciences Discuss., doi:10.5194/bg-2017-114, 2017
Manuscript under review for journal Biogeosciences
Discussion started: 28 April 2017

159 The paper is organized as follows. Model, Data and Methodology are detailed in Section
160 2. The spatially inhomogeneous Zc derived out of the new parameterization and its impact in
161 simulated seasonality of biology and carbon cycle are detailed in Section 3. Further results and
162 discussion are followed in Section 4 and a conclusion is given in Section 5.

163 **2. Model, Data and Methods**

164 **2.1. Model**

165 The study utilizes the Offline Ocean Tracer Transport Model (OTTM) (Valsala et al., 2008)
166 coupled with OCMIP biogeochemistry model (Raymond Najjar and James Orr, 1998). OTTM
167 does not compute currents and stratifications (i.e., temperature and salinity) on its own. It is
168 capable of accepting any ocean model or data-assimilated product as physical drivers. The
169 physical drivers prescribed include 4-dimensional currents (u,v), temperature, salinity, and 3-
170 dimensional mixed layer depth, surface freshwater and heat fluxes, surface wind stress and sea
171 surface height. The resolution of the model setup is similar to the parent model from which it
172 borrows the physical drivers. With the given input of Geophysical Fluid Dynamics Laboratory
173 (GFDL) reanalysis data, the zonal and meridional resolutions are 1^o with 360 grid points
174 longitudinally and 1^o at higher latitudes but having a finer resolution of 0.8^o in the tropics, with
175 200 grid points, respectively. The model has 50 vertical levels with 10m increment in the upper
176 225m and stretched vertical levels below 225m. The horizontal grids are formulated in spherical
177 co-ordinates and vertical grids are in z levels. The model employs a B-grid structure in which the
178 velocities are resolved at corners of the tracer grids. The model uses a centered-in-space and
179 centered-in- time (CSCT) numerical scheme along with an Asselin-Robert filter (Asselin., 1972)
180 to control the ripples in CSCT.

Biogeosciences Discuss., doi:10.5194/bg-2017-114, 2017
Manuscript under review for journal Biogeosciences
Discussion started: 28 April 2017

181 The tracer concentration (C) evolves with time as

182 $$\frac{\partial C}{\partial t} + U.\nabla_H C + W\frac{\partial C}{\partial z} = \frac{\partial}{\partial z}K_z\frac{\partial}{\partial z}C + \nabla_H.(K_h\nabla_H C) + \Phi \qquad (1)$$

183 where ∇_H is the horizontal gradient operator, U and W are the horizontal and vertical velocities
184 respectively. K_z is the vertical mixing coefficient, and K_h is the two-dimensional diffusion
185 tensor. Φ represents any sink or source due to the internal consumption or production of the
186 tracer as well as the emission or absorption of fluxes at the ocean surface. Here, the source and
187 sink term are provided through the biogeochemical model. Vertical mixing is resolved in the
188 model using K- profile parameterization (KPP) (Large et al., 1994).

189 In addition to KPP, the model uses a background vertical diffusion reported by Bryan and Lewis
190 (Bryan and Lewis., 1979) in order to represent the convention and mixing that happens in a time
191 scale of a few days. For horizontal mixing model incorporates Redi fluxes (Redi., 1982) and GM
192 fluxes (Gent and Mcwilliams., 1990) which accommodate the eddy induced variance from the
193 mean in the tracer transport. A weak Laplacian diffusion is also included in the model for
194 computational stability where sharp gradient of concentration occurs.

195 The biogeochemical model used in the study is based on the OCMIP – II protocol as
196 stated above. The main motivation of OCMIP–II model design is to simulate the ocean carbon
197 cycle with reductionist approach to ocean biology using appropriate biogeochemical
198 parameterizations. The major advantage of the OCMIP – II protocol is (i) it reproduces the first
199 order carbon cycle and the associated elemental cycles in the ocean reasonably well and (ii) it is
200 much easier to implement and computationally efficient than the explicit ecosystem models. The
201 present version of the model has five prognostic variables coupled with the circulation field, viz.,
202 inorganic phosphate (PO_4^{3-}), dissolved organic phosphorous (DOP), oxygen (O_2), dissolved

Biogeosciences Discuss., doi:10.5194/bg-2017-114, 2017
Manuscript under review for journal Biogeosciences
Discussion started: 28 April 2017

inorganic carbon (DIC) and alkalinity (ALK). In order to retrieve the accurate spatial and temporal distribution of CO_2 flux and pCO_2, the model uses a "nutrient restoring" approach (Najjar et. al., 1992, Anderson and Sarmiento., 1995) for biological production. The basic currency for biological production in the model is phosphate because of the availability of a more extensive database and to eliminate the complexities associated with nitrogen fixation and denitrification. The biogeochemical dynamics implemented in the model are given Appendix-A

The air – sea CO_2 flux in the model is estimated by,

$$F = K_w \, \Delta \, pCO_2 \qquad (2)$$

where K_w is gas transfer velocity and $\Delta \, pCO_2$ is the difference in partial pressure of carbon dioxide between the ocean and atmosphere. The design and validation of the physical model is reported by Valsala et. al.,(2008, 2010) and biogeochemical design by Najjar and Orr (1998).

2.2. Data

The present setup of the model uses ocean reanalysis products based on MOM–4 (Modular Ocean Model) developed by GFDL (Chang et. al., 2012). Monthly data from 1961 to 2010 were utilized in the present study. For validating the results observational datasets of CO_2 flux and pCO_2 were taken from Takahashi et al., (2009). Satellite derived Net Primary Production data were taken from Sea-viewing Wide Field of view sensor (SeaWiFS) Chl-a product, calculated using Vertically Generalized Production Model (VGPM) (Behrenfeld and Falkowski, 1997). The initial conditions for PO_4 and O_2 were taken from World Ocean Atlas (Conkright et al., 1994). Initial conditions for DIC and ALK were taken from the Global Ocean Data Analysis Project (GLODAP) dataset. The data sources and citations are given in the Acknowledgement.

Biogeosciences Discuss., doi:10.5194/bg-2017-114, 2017
Manuscript under review for journal Biogeosciences
Discussion started: 28 April 2017

A spin-up for 50 years from the given initial conditions are performed with the climatological physical drivers. Because the initial conditions were provided from a mean state observed climatology this duration of spin-up is sufficient to reach statistical equilibrium in the upper 1000 m (Le Quere et al., 2000). Atmospheric pCO_2 has been set to a value from the 1950s in the spin-up run for calculating the air-sea CO_2 exchange. A seasonal cycle of atmospheric pCO_2 has been prescribed.

After the spin-up, an interannual simulation for 50 years from 1961 to 2010 has been carried out with the corresponding observed atmospheric pCO_2 described in Keeling et al, (1995). The first five years of the interannual run were looped five times through the physical fields of 1961 repeatedly for a smooth merging of the spin-up restart to the interannual physical variables. Since the study is focused only on bias corrections to seasonal cycle with a variable Zc, a model climatology has been constructed from 1990 to 2010. This includes the anthropogenic increase of oceanic DIC in the climatological calculation and is comparable with the Takahashi et al. (2009) observations.

Additional two sensitivity experiments have been performed separately by providing annual mean currents or temperatures as drivers over selected regions of the basin for segregating the role of varying compensation depth (varZc) in improving the seasonality of carbon cycle and biological production. The model driven with annual mean currents suppress the effect of upwelling by muting the ekman divergence over the region of interest. On the other hand, the model forced with annual mean temperatures suppresses the cooling effect of upwelling. This will highlight the effect of new parameterization in simulating seasonality of carbon cycle and biological production. A smoothing technique with linear interpolation ($u = u(1-x) + \bar{u}x$) is applied to the offline-data in order blend the annual mean fields ($\bar{u}$)

Biogeosciences Discuss., doi:10.5194/bg-2017-114, 2017
Manuscript under review for journal Biogeosciences
Discussion started: 28 April 2017

given to the selected region with the rest of the domain (u) in order to reduce a sudden transition at the boundaries.

2.3. Compensation depth (Z_c) parameterization

The OCMIP – II simulation protocol separates the production and consumption zones by a depth termed as compensation depth (Z_c); the depth at which photosynthesis is equal to respiration of the photosynthetic community (Smetacek and Passow., 1990). The light intensity at compensation depth is compensation irradiance (I_c) with larger values at higher temperatures since respiration is temperature dependent (Parsons et. al., 1984, Ryther, 2003). We define a spatially and temporally varying compensation depth (hereinafter varZc) as a depth where solar radiation (attenuated by surface Chl-a, Jerlov et al., 1976) reaches a minimum value of 10 W m^{-2}. In this way the varZc has both spatio-temporal variability of light as well as Chl-a data. The Chl-a is given as monthly climatology as constructed from the satellite data. Observations show that the primary production reduces rapidly to 20% or less of the surface value below a threshold of 10 W m^{-2} (Parsons et.al., 1984, Ryther, 2003). Figure 2 compares the scatter of average relative photosynthesis within varZc as a function of solar radiation for the Indian Ocean. This encapsulate the corresponding curve from the observations for the major phytoplankton species in the ocean such as diatoms, green algae and dinoflagellates (Ryther et al., 1956, 2003, Parsons et al., 1984). The model permits 100% relative photosynthesis for radiation above 50 W m^{-2}. However the availability of phosphate concentration in the model act as an additional limiter for production which indirectly represents the photoinhibition at higher irradiance, for example oligotrophic gyres.

Biogeosciences Discuss., doi:10.5194/bg-2017-114, 2017
Manuscript under review for journal Biogeosciences
Discussion started: 28 April 2017

3. **Results and Discussions**

The inclusion of seasonality in Zc by way of parameterizing varZc leads to a remarkable spatio-temporal variability in compensation depth (Figure 3). The compensation depth over the Arabian Sea varies from 10m to 25m during DJF and deepens up to 45m during MAM in par with incoming solar radiation. During the monsoon season (JJAS), the compensation depth again shoals to 10m-35m due to the attenuation of solar radiation by the increased biological production (Chl-a). During Oct–Nov the Zc slightly deepens as compared to JJAS.

The Bay of Bengal compensation depth deepens from 35m to 40m during DJF and further deepens to 50m during MAM when the solar radiation is maximum and biological production is minimum (Prasannakumar et al., 2002). Further reduction of compensation depth can be seen through JJAS as a result of reduction in solar radiation during monsoon cloud cover. The Zc during Oct – Nov is on an average of 35m. However, caution is needed since the Bay of Bengal is dominated by freshwater forcing from rivers and precipitation and temperature inversions occur routinely (Howden and Murtugudde., 2001, Vinayachandran et. al., 2013). The impact of these factors on compensation depth variability is not clear and is not addressed here.

The equatorial Indian Ocean can be seen as a belt of 40m-45m deep compensation depth throughout the season except for JJAS. During JJAS, a shallow compensation depth is seen near the coastal Arabian Sea (around 10m to 35m) presumably due to the coastal Chl-a blooms. Deep compensation depth off the coast of Sumatra (~ 40m to 50m) is found during JJAS. Java-Sumatra coastal upwelling is centered on September-Nov (Susanto et al., 2001) and upwelling originates at around 100m deep (Xing et al., 2012).

Biogeosciences Discuss., doi:10.5194/bg-2017-114, 2017
Manuscript under review for journal Biogeosciences
Discussion started: 28 April 2017

292 Southward of 10°S in the oligotrophic gyre region, the compensation depth varies from 40m to
293 more than 60m throughout the year. A conspicuous feature observed while parameterizing the
294 solar radiation and Chl-a dependent Zc is that its maximum value never crosses 75 m especially
295 in the Indian Ocean which is the value specified in OCMIP-II models. The cutoff depth of 75 m
296 in OCMIP-II is obtained from observing the seasonal variance in the oxygen data (Najjar and
297 Keeling, 1997) as an indicator of production zone. However, parameterizing a production zone
298 based on optimum solar radiation and Chl-a (Parsons et al., 1984) predicts a production zone
299 and its variability that is largely less than 75 m. The consequence of this in the seasonality of the
300 modeled carbon cycle is illustrated as follows.

301 **3.1. Simulated seasonal cycle of pCO_2 and CO_2 fluxes**

302 The annual mean biases in simulated CO_2 fluxes and pCO_2 were evaluated by comparing
303 with Takahashi et al., (2009) observations (Figure 4). The model biases are significantly reduced
304 with the implementation of varying Z_c compared to that of the constant Z_c. A notable reduction in
305 pCO_2 bias (by ~ 10µatm) is observed along the WAS region [Figure (4d)].

306 In order to address the role of the new biological parameterization of a variable
307 compensation depth, we extended our study by choosing four key regions where the biological
308 production and CO_2 fluxes are prominent in the Indian Ocean with additional sensitivity
309 experiments (see Introduction and references therein). The boxes we considered are, (1) Western
310 Arabian Sea (WAS) [40°E:65°E, 5°S:25°N] (2) Sri Lanka Dome (SLD) [81°E:90°E, 0°:10°N] (3)
311 Seychelles-Chagos Thermocline Ridge (SCTR) [50°E:80°E, 5°S:10°S] (4) Sumatra Coast (SC)
312 [90°E:110°E, 0°:10°S; Figure 1]. The seasonal variations of Zc over these selected key regions

Biogeosciences Discuss., doi:10.5194/bg-2017-114, 2017
Manuscript under review for journal Biogeosciences
Discussion started: 28 April 2017

313 are shown in Figure 5. A detailed analysis of CO_2 fluxes, pCO_2, biological export and new
314 production for these key regions are presented below.

315

316 **3.2. Western Arabian Sea (WAS) region**

317 The WAS Zc has a double peak pattern over the annual cycle. Over the February-March
318 period Z_c deepens up to a maximum of 43.85 ± 2.3 m into March and then shoals to 25.75 ± 1.5
319 m (Fig 5) during the monsoon period (uncertainty represents the interannual standard deviations
320 of monthly data from 1990-2010). This shoaling of compensation depth during the monsoon
321 indicates the potential ability of the present biological parameterization to capture the wind
322 driven upwelling related production in the WAS. During the post monsoon period, the second
323 deepening of compensation depth occurs during November with a maximum depth of 34.91 ±
324 2.2 m. The ability to represent the seasonality of biological production zone renders a unique
325 improvement in CO_2 flux variability especially in the WAS region in comparison to the OCMIP-
326 II experiments (Orr et al, 2003, Figure (6a)).

327 OCMIP –II simulations with a constant Z_c of 75 m underestimate the CO_2 flux when
328 compared to the observations of Takahashi et al. (2009). This underestimation is clearly visible
329 during monsoon period. Our simulations with the present biological parameterization having a
330 spatially and temporally varying compensation depth results in a better seasonality of CO_2 flux
331 when compared with Takahashi et al. (2009) observations (Figure 6a). The improvement brought
332 about the varying Zc scheme is able to represent the seasonality of CO_2 flux especially during the
333 monsoon period, when wind driven upwelling is dominant. Obviously the role of the biological
334 and solubility pumps have to be deciphered in this context.

Biogeosciences Discuss., doi:10.5194/bg-2017-114, 2017
Manuscript under review for journal Biogeosciences
Discussion started: 28 April 2017

335 The CO_2 flux during July from observations, constZc simulations and varZc simulations are
336 3.09 mol m^{-2} yr^{-1}, 1.82 ± 0.4 mol m^{-2} yr^{-1} and 3.10 ± 0.5 mol m^{-2} yr^{-1}, respectively. Southwesterly
337 wind-driven upwelling over the WAS especially off Somali coast (Smith & Codispoti, 1980,
338 Schott, 1983, Smith, 1984) and Oman (Bruce, 1974, Smith &Bottero, 1977, Swallow, 1984,
339 Bauer et al, 1991), pulls nutrient-rich subsurface waters closer to the surface while the available
340 turbulent energy due to the strong winds leads to mixed layer entrainment of the nutrients
341 resulting in a strong surface phytoplankton bloom (Krey & Babenerd, 1976, Banse, 1987, Bauer,
342 1991, Brock et al, 1991). This regional bloom extends over 700 km offshore from the Omani
343 coast due to upward Ekman pumping driven by strong, positive wind-stress curl to the northwest
344 of the low level jet axis and the offshore advection (Bauer et. al., 1991, Brock et al., 1991, Brock
345 & McClain, 1992a, b, Murtugudde and Busalacchi., 1999) resulting in strong outgassing of CO_2
346 flux and an enhanced pCO_2 in the western Arabian Sea region (Valsala and Maksyutov, 2013,
347 Sarma et al., 2002). The seasonal mean CO_2 flux during the southwest monsoon period (JJAS)
348 for constZc simulations and varZc simulations are 1.44 ± 0.2 mol m^{-2} yr^{-1} and 2.31 ± 0.4 mol m^{-2}
349 yr^{-1}, respectively. The biological parameterization of varying compensation depth considerably
350 improves the average CO_2 flux during the monsoon period by 0.86 ± 0.1 mol m^{-2} yr^{-1}. The annual
351 mean CO_2 flux from observations, constZc simulations and varZc simulations are 0.94 mol m^{-2}
352 yr^{-1}, 0.80 ± 0.17 mol m^{-2} yr^{-1} and 1.07 ± 0.2 mol m^{-2} yr^{-1}, respectively. The annual mean CO_2 flux
353 improved by 0.27 ± 0.05 mol m^{-2} yr^{-1}.

354 Seasonality in pCO_2 also shows a remarkable improvement during the southwest monsoon
355 period [Figure (6b)]. The pCO_2 with ConstZc is considerably lower at a value of 385.22 ± 3.5
356 µatm during June compared to observational values of 392.83 µatm. However, varZc simulations
357 perform better in terms of pCO_2 variability. The peak value of pCO_2 reaches up to 405.42 ± 5.8

Biogeosciences Discuss., doi:10.5194/bg-2017-114, 2017
Manuscript under review for journal Biogeosciences
Discussion started: 28 April 2017

358 µatm. The seasonal mean pCO_2 during the southwest monsoon period from observations,
359 constZc simulations and varZc simulations are 397.58 µatm, 389.18 ± 3.6 µatm and 399.95 ± 5.0
360 µatm, respectively. The improvement in pCO_2 brought about by varZc simulations is 10.76 ± 1.3
361 µatm compared to the constZc simulations. This inherently says that constZc simulations fail to
362 capture the pCO_2 driven by upwelling during southwest monsoon, meanwhile varZc simulations
363 are demonstrably better in representing this seasonal increase. The annual mean pCO_2 from
364 observations, constZc and varZc simulations are 394.69 µatm, 389.62 ± 3.9 µatm and 391.19 ±
365 4.7 µatm, respectively. However it is worth mentioning that there are parts of the year where the
366 constant Zc performs better compared to varying Zc. For instance during MAM as well as in
367 November, the constZc simulations yielded a better comparison with the observed pCO_2 whereas
368 varZc simulations yield a reduced magnitude of pCO_2. This may well indicate the biological vs
369 solubility pump controls on pCO_2 during the intermonsoons. The role of mesoscale variability in
370 the ocean dynamics may also play a role (Valsala and Murtugudde, 2015) Nevertheless during
371 the most important season (JJAS) when the pCO_2, CO_2 fluxes and biological production are
372 found to be dominant in the Arabian Sea, the varying Zc produces a better simulation.

373 The improvement shown by the implementation of new biological parameterization in the
374 simulations of CO_2 flux and pCO_2 can be answered by further analysis of the model biological
375 production. Figure 7 shows the comparison of model export production and new production with
376 observational export production from satellite-derived NPP for constZc and varZc simulations.
377 The model export production in the constZc simulations is much weaker when compared to
378 varZc simulations. The varZc simulations have improved the model export production.
379 Theoretically, the new and export productions in the model should be in balance with each other

Biogeosciences Discuss., doi:10.5194/bg-2017-114, 2017
Manuscript under review for journal Biogeosciences
Discussion started: 28 April 2017

(Eppley and Peterson, 1979). ConstZc export production is much weaker than new production and it is not in balance. In contrast the varZc simulation yields a nice balance among them.

Comparing with the observational export production which peaks in August at a value of 154.78 g C m^{-2} yr^{-1}, the varZc simulated export and new productions peak at a value of 160.44 ± 20.4 g C m^{-2} yr^{-1} and 167.18 ± 24.0 g C m^{-2} yr^{-1}, respectively but in July. A similar peak can be observed in constZc simulated new production as well at a value of 178.19 ± 28.0 g C m^{-2} yr^{-1}. This apparent shift of one month during JJAS in the model export production as well as in the new production is noted as a caveat in the present set up which will need further investigation. Arabian Sea production is not just limited by nutrients but also the dust inputs (Wiggert and Murtugudde., 2006). The dust induced primary production in the WAS especially over the Oman coast is noted during August (Liao et. al., 2016). The mesoscale variability in the circulation and its impact on production and carbon cycle are also a limiting factor in this model as noted above.

The seasonal mean export production during the southwest monsoon period from satellite-derived estimate is 123.57 g C m^{-2} yr^{-1}, whereas for constZc and varZc simulations it is 84.81 ± 16.0 g C m^{-2} yr^{-1} and 147.19 ± 23.8 g C m^{-2} yr^{-1}, respectively. The new biological parameterization strengthened the model export production by 62.38 ± 7.8 g C m^{-2} yr^{-1} for the southwest monsoon period, which is over a 70% increase. This indicates a considerable impact of the biological pump in the model simulated CO_2 flux and pCO_2 over the WAS. For constZc simulations, the computed new production is slightly higher (150.84 ± 27.9 g C m^{-2} yr^{-1}) than that of varZc (133.03 ± 19.5 g C m^{-2} yr^{-1}). The annual mean export production from observations, constZc and varZc simulations are 94.31 g C m^{-2} yr^{-1}, 77.41 ± 15.1 g C m^{-2} yr^{-1} and 122.54 ± 25.2 g C m^{-2} yr^{-1}, respectively.

Biogeosciences Discuss., doi:10.5194/bg-2017-114, 2017
Manuscript under review for journal Biogeosciences
Discussion started: 28 April 2017

To understand how the varying compensation depth parameterization strengthened the export production in the model, we analyzed the phosphate profiles. It appears that the varZc parameterization allows more phosphate concentration (Figure 8a,b) in the production zone and thereby increases the corresponding biological production (Figure 8c, d). The net export production in the model during JJAS is consistent with the satellite data (Figure 8d, see also Figure 7a). However, in the constZc case the exports are rather 'flat' throughout the season with imperfect representation of seasonal biological export. The Table 1-4 summarizes all the values discussed here.

3.3 SriLanka Dome (SLD) Region

The seasonal variation in the compensation depth for the SLD has a similar pattern as that of the WAS. The compensation depth deepens to its maximum during March up to 45.23 ± 0.3 m and reaches its minimum during the following monsoon period at 30.79 ± 1.5 m [Figure (5)]. The similarities of varZc between WAS and SLD indicate that they both are under similar cycles of solar influx and biological production. The SLD chl-a dominates only up to July (Vinayachandran et al., 2004) which explains why production with varZc increase earlier compared to the WAS which occurs during August-October.

The seasonality in CO_2 flux and pCO_2 were compared with Takahashi et al., (2009) observations [Figure (9)]. The varZc results in a slight improvement in CO_2 flux when compared with constZc [Figure (9a)]. However both constZc and varZc simulations underestimate the magnitude of CO_2 flux when compared with observations. The seasonal mean CO_2 flux during

Biogeosciences Discuss., doi:10.5194/bg-2017-114, 2017
Manuscript under review for journal Biogeosciences
Discussion started: 28 April 2017

424 the monsoon period is 1.79 mol m^{-2} yr^{-1} from observations, which means SLD region is a source
425 of CO_2. But the mean values of constZc and varZc simulations yield flux values of -0.008 ± 0.2
426 mol m^{-2} yr^{-1} and 0.24 ± 0.2 mol m^{-2} yr^{-1}, respectively. The constZc simulations misrepresent the
427 SLD region as a sink of CO_2 during monsoon period which is opposite to that of observations.
428 The varZc simulations correct this misrepresentation to a source albeit at a smaller magnitude by
429 0.24 ± 0.09 mol m^{-2} yr^{-1} for the monsoon period. Compared to observations, the varZc case
430 underestimates the magnitude of JJAS mean by 1.55 mol m^{-2} yr^{-1}.

431 The annual mean CO_2 fluxes for constZc and varZc simulations are -0.02 ± 0.1 mol m^{-2} yr^{-1}
432 and 0.10 ± 0.2 mol m^{-2} yr^{-1}, respectively. The varZc parameterization leads to an improvement of
433 0.13 ± 0.1 mol m^{-2} yr^{-1} in the annual mean CO_2 flux when compared with constZc simulations.
434 The observational annual mean of CO_2 flux is 0.80 mol m^{-2} yr^{-1} which is highly underestimated
435 by both simulations. This indicates a regulation of biological production of the region by varZc
436 which makes this region a source of CO_2 during monsoon. The role of the solubility pump may
437 also be underestimated due to the biases in the physical drivers and the lack of mesoscale eddy
438 activities in these simulations (Prasanna Kumar et. al., 2002, Valsala and Murtugudde., 2015).

439 The seasonality of pCO_2 [Figure 9(b)] especially in the monsoon period has significantly
440 improved. The mean pCO_2 during the monsoon season from observation over the SLD region is
441 382.44 µatm. The seasonal mean pCO_2 during monsoon period for constZc and varZc
442 simulations are 371.67 ± 6.04 µatm and 379.24 ± 8.9 µatm, respectively. The annual mean pCO_2
443 from observations, constZc and varZc simulations are 380.21 µatm, 370.76 ± 6.1 µatm and
444 374.94 ± 9.6 µatm, respectively. varZc simulations improve the JJAS mean pCO_2 by 7.56 ± 2.8
445 µatm and the annual mean pCO_2 by 4.18 ± 3.5 µatm, which is reflected in CO_2 flux as well. This

Biogeosciences Discuss., doi:10.5194/bg-2017-114, 2017
Manuscript under review for journal Biogeosciences
Discussion started: 28 April 2017

446 is likely due to the impact of new biological parameterization in capturing the episodic upwelling
447 in the SLD region which is further investigated by looking at its biological production.

448 The SLD biological production is highly exaggerated by the model for both constZc and
449 varZc simulations (Figure 10a,b). The seasonal mean biological export for the monsoon period is
450 51.54 g C m^{-2} yr^{-1} as per satellite-derived estimates. However, the constZc and varZc simulations
451 overestimate it by 167.71 ± 59.04 g C m^{-2} yr^{-1} and 151.51 ± 46.4 g C m^{-2} yr^{-1}, respectively. This
452 exaggerated export is visible in climatological annual means where for constZc and varZc
453 simulations they are 144.43 ± 49.8 g C m^{-2} yr^{-1} and 156.08 ± 43.8 g C m^{-2} yr^{-1}, respectively.

454 For constZc simulations, new production is overestimated from March to Oct when
455 compared to the observations and second peak is observed in November (Figure 10a). But the
456 overestimate in new production with varZc is observed only during JJAS period by a value of
457 26.23 g C m^{-2} yr^{-1}. For the SLD region the varZc parameterization overestimates the export
458 production but minimizes the excess new production, especially in the monsoon period by 64.15
459 ± 36.4 g C m^{-2} yr^{-1}. This indicates that the varZc parameterization is somewhat successful in
460 capturing the upwelling episode during monsoon over SLD. All values are summarized in Table
461 1-4.

462 **3.4 Sumatra Coast (SC) region**

463 The seasonal variation in the compensation depth over the SC region lies between 40 m and
464 46 m [Figure (5)]. The seasonal maximum occurs during JFM, especially in March with a depth
465 of 45.5 m. During the monsoon period the compensation depth shoals slightly, with a minimum
466 of 41.1 m in July. The variation in Z_c is relatively small as compared to the other regions which
467 is consistent with its relatively low production throughout the year.

Biogeosciences Discuss., doi:10.5194/bg-2017-114, 2017
Manuscript under review for journal Biogeosciences
Discussion started: 28 April 2017

468 The seasonality of CO_2 flux and pCO_2 captured by constZc and varZc simulations are shown
469 in Figure 11(a, b). The varZc simulations overestimate both CO_2 flux and pCO_2 especially during
470 the monsoon. It is found that the constZc simulations are better compared to varZc simulations.
471 The varZc simulations overestimate the seasonal mean CO_2 flux and pCO_2 by 1.19 mol m^{-2} yr^{-1}
472 and 29.61 µatm, respectively, compared to observations (Table 1). However, constZc produces a
473 better estimate compared with observations for CO_2 flux and pCO_2. The constZc simulations
474 deliver a better annual mean than varZc (Table 1,2). The annual mean bias in constZc and varZc
475 simulations for CO_2 flux is -0.0033 mol m^{-2} yr^{-1} and 0.31 mol m^{-2} yr^{-1}, respectively. Similarly
476 pCO_2 bias is 1.95 µatm and 9.07 µatm for constZc and varZc simulations.

477 Biological production simulated by the model in the SC explains the overestimation of CO_2
478 flux and pCO_2 (Figure 12). Both constZc and varZc simulations greatly overestimates export
479 production in the model. But a small enhancement in the new production during JJAS in constZc
480 case is an indicator of upwelling episodes. The seasonal mean new production during the
481 monsoon from constZc and varZc are 63.64 ± 30.9 g C m^{-2} yr^{-1} and 78.11 ± 29.1 g C m^{-2} yr^{-1},
482 respectively (Table 4). The seasonal mean export production during the monsoon from
483 observation is 58.87 g C m^{-2} yr^{-1} (Table 3). ConstZc simulations represent a better new
484 production, which is seen as a relatively small exaggeration of CO_2 flux and pCO_2. The
485 biological response off SC is found to be better with constZc which is in contradiction to a
486 general improvement found with varZc in the other regions examined here. Such discrepancies
487 over the SC could be due to the effect of Indonesian Throughflow (Bates et al., 2006) which is
488 not completely resolved in the model due to coarse spatial resolution.

489

Biogeosciences Discuss., doi:10.5194/bg-2017-114, 2017
Manuscript under review for journal Biogeosciences
Discussion started: 28 April 2017

3.5 Seychelles-Chagos Thermocline Ridge (SCTR) region

The SCTR is a unique upwelling region with a prominent variability in air-sea interactions (Xie et al., 2002). Wind-driven mixing and upwelling of subsurface nutrient rich water play a major role in biological production of this region (Dilmahamod et al., 2016). The seasonal cycle in the compensation depth is shown in figure 5. The maximum compensation depth occurs in November at about 44.94 m and the minimum at 33.2 m in July. The shoaling of compensation depth during the monsoon period shows that the biological parameterization captures the upwelling response over this region.

The seasonality of CO_2 flux and pCO_2 are shown in Figure 13. The Takahashi observations of CO_2 flux shows a peak in June with outgassing of CO_2 during the upwelling episodes. However, both constZc and varZc simulations underestimate this variability. The seasonality of CO_2 flux in varZc shows a significant improvement when compared to constZc simulations, but underestimated when compared to observations. The seasonal mean CO_2 flux during the monsoon for constZc and varZc simulations are 0.82 mol m^{-2} yr^{-1}, -0.32 ± 0.3 mol m^{-2} yr^{-1} and -0.05 ± 0.4 mol m^{-2} yr^{-1}, respectively. This represents a reduction in seasonal mean sink of CO_2 flux in the SCTR region during the monsoon by 0.27 ± 0.1 mol m^{-2} yr^{-1} bringing it closer to a source region (see Table 1 for details).

The improvement brought about in CO_2 flux is supported by the seasonal cycle in pCO_2 . Based on observations, seasonal mean of pCO_2 with constZc during JJAS is underestimated by 11.47 µatm, varZc simulations underestimate it by 6.45 µatm. So it is evident that varZc simulations capture the upwelling episodes better, marked by a greater pCO_2 during JJAS period. However, the magnitude of pCO_2 is still underestimated compared to observations (Table 2).

Biogeosciences Discuss., doi:10.5194/bg-2017-114, 2017
Manuscript under review for journal Biogeosciences
Discussion started: 28 April 2017

512 Figure 14 shows the biological production of constZc and varZc simulations for SCTR. It is
513 clear that both simulations overestimate the export production and underestimate the new
514 production. The JJAS mean export production from observations, constZc and varZc are 51.08 g
515 C m^{-2} yr^{-1}, 57.39 ± 14.2 g C m^{-2} yr^{-1} and 99.23 ± 29.8 g C m^{-2} yr^{-1}, respectively. The varZc
516 simulations exaggerate the model export production by 48.14 g C m^{-2} yr^{-1}.The varZc simulations
517 improve the JJAS mean new production by 1.14 ± 2.2 g C m^{-2} yr^{-1} (Table 4). This slight
518 improvement in the model new production especially during the monsoon period signals that the
519 spatially and temporally varying compensation depth better captures the upwelling over SCTR.
520 Considering the annual mean values of model export and new production, constZc simulations
521 are reasonably faithful to observations.

522 The underestimation of CO_2 and pCO_2 as well as the exaggeration of model export
523 production and a slight overestimate in model new production may be due to two reasons. (1)
524 SCTR is a strongly coupled region with remote forcing of the mixed layer – thermocline
525 interactions (Zhou et al., 2008) which can affect the seasonality in biological production that the
526 model may not be resolving reasonably (2) The bias associated with physical drivers, especially
527 wind stress may underestimate the CO_2 flux as well biological production. A similar
528 overestimation of biological production was also reported in a coupled biophysical model
529 (Dilmahamod et. al., 2016).

530 Table 1 – 4 shows the entire summary of seasonal and annual mean CO_2 flux, pCO_2 and
531 biological production reported in Section 3.

532

533

Biogeosciences Discuss., doi:10.5194/bg-2017-114, 2017
Manuscript under review for journal Biogeosciences
Discussion started: 28 April 2017

4. Sensitivity Simulations

From the analysis of four major upwelling regions over Indian Ocean, it is evident that the biological parameterization of spatio-temporally varying compensation depth better captures upwelling episodes and thus it enhances the model export production. This is clearly visible over the WAS. In order to quantify how much the varZc parameterization contributed to seasonality of carbon cycle, two additional sensitivity simulations were carried out; (1) with annual mean offline currents and (2) annual mean offline temperatures with the notion of suppressing the dynamical and thermodynamical effects of seasonal upwelling over the WAS (see Section 2 for details). The focus on this region is motivated by its prominence as the most productive zone of the Indian Ocean. Moreover, the improvement in the biological processes in the model by the varZc parameterization is best captured in this region. The results are discussed in detail in the following subsections.

4.1 Impact of varZc parameterization in seasonality of carbon cycle with annual mean currents.

To quantify the impact of varZc parameterization, the model is forced with annual mean currents only over the WAS with unaltered currents in the rest of the ocean. The hypothesis is that the muting of the seasonal variability of Ekman divergence removes the upwelling and the biological pump contribution to production and carbon cycle. The comparison of constZc and varZc then allows us to decipher the impact of varZc on capturing the impacts of upwelling on biological production and the carbon cycle. The smooth blending of currents at the boundary of the WAS domain is achieved by a linear smoothing function as given in Section 2.

Biogeosciences Discuss., doi:10.5194/bg-2017-114, 2017
Manuscript under review for journal Biogeosciences
Discussion started: 28 April 2017

556 The model biological responses (inferred by comparing with the control run) in terms of the
557 CO_2 flux shows a flat pattern over the monsoon period for constZc simulations [Figure 15(a)].
558 While the varZc simulations forced with the annual mean currents shows an enhanced CO_2 flux
559 indicating the outgassing of CO_2 flux in the WAS due to wind-driven upwelling (Figure 15(b)).
560 This qualitatively shows that the spatially and temporally varying compensation depth itself has
561 improved the seasonality in the biological processes (export and new production) and captured
562 the upwelling episodes during the monsoon. The varZc parameterization is responsible for
563 improvement of 0.48 ± 0.04 mol m^{-2} yr^{-1} and 0.13 ± 0.02 mol m^{-2} yr^{-1}during JJAS seasonal and
564 annual mean CO_2 flux, respectively. This improves the overall model CO_2 flux in the control run
565 especially in July (Figure 15(b)).

566 Similar improvements were also noticed in pCO_2 (Figure 16). In the constZc simulations
567 with annual mean currents, the pCO_2 dips down during JJAS monsoon period which indicates
568 the inadequacy of constZc in capturing the upwelling enriched pCO_2 difference (Figure 16a, b).
569 The varZc simulation slightly modifies the pCO_2 in the 'right' direction during JJAS despite the
570 annual mean currents.

571 The export production and the new production in the model explain the modification of
572 CO_2 flux and pCO_2 by varZc parameterization. The biological export production is highly
573 underestimated in the constZc simulations forced with annual mean currents while the varZc
574 simulations captures the seasonal upswing in production (Figure 17). The improved JJAS mean
575 and annual mean export production by 43.51 ± 8.6 g C m^{-2} yr^{-1} and 30.28 ± 13.7 g C m^{-2} yr^{-1},
576 respectively is a clear indication of the positive impacts of a variable Zc. Similarly the
577 improvement in JJAS mean and annual mean new production (Figure 18) from varZc simulated
578 with annual mean currents were 17.39 ± 0.8 g C m^{-2} yr^{-1} and 14.81 ± 0.1 g C m^{-2} yr^{-1},

Biogeosciences Discuss., doi:10.5194/bg-2017-114, 2017
Manuscript under review for journal Biogeosciences
Discussion started: 28 April 2017

579 respectively. In short the varZc biological parameterization improves the export and new
580 productions in the model. This helps the model to capture the upwelling episodes over the study
581 regions. Table 5 summarizes all the results of biological sensitivity runs.

582

583 **4.2 Impact of varZc parameterization in seasonality of carbon cyle with annual**
584 **mean temperatures.**

585 Using the annual mean temperature over the WAS, we are suppressing the cooling effect of
586 temperature due to upwelling and quantifying how much the model seasonality is improved by
587 means of varZc parameterization. (see Section 2 for details). The varZc simulations forced with
588 annual mean SST has greater JJAS mean and annual mean CO_2 flux by 0.88 ± 0.1 mol m^{-2} yr^{-1}
589 and 0.28 ± 0.07 mol m^{-2} yr^{-1}, respectively (Figure 19 and Table 6). For a given annual mean SST
590 the solubility pump largely controls the CO_2 emission during JJAS if a variable Zc is prescribed,
591 likely by the enrichment in the DIC (inferred from Figure 8b). Similarly the improvement in
592 pCO_2 (Figure 20) with varZc simulation is also remarkable. The JJAS mean and annual mean
593 improvements from the implementation of varZc are 11.05 ± 1.9 µatm and 1.91 ± 1.4 µatm,
594 respectively. The detailed quantification of CO_2 and pCO_2 responses for this experimental setup
595 is given in Table 6. The above analysis adds supporting evidence that the varZc simulations
596 strengthen the seasonality of the model compared to the constZc case. This is presumably
597 accomplished by the more accurate compensation depth and production zone implied with a
598 variable Zc.

599

600

Biogeosciences Discuss., doi:10.5194/bg-2017-114, 2017
Manuscript under review for journal Biogeosciences
Discussion started: 28 April 2017

5. Summary and Conclusions

A spatially and temporally varying compensation depth parameterization as a function of solar radiation and Chl-a is implemented in the biological pump model of OCMIP-II for a detailed analysis of biological fluxes in the upwelling zones of the Indian Ocean. The varZc parameterization improves the seasonality of model CO_2 flux and pCO_2 variability, especially during the monsoon period. Significant improvement is observed in the WAS where monsoon wind-driven upwelling dominates biological production. The magnitude of CO_2 flux matches with observations, especially in July when monsoon winds are at their peak. Monsoon triggers upwelling in SLD as well which acts as a source of CO_2 to the atmosphere. The seasonal and annual mean are underestimated with constZc and the SLD is reduced to a sink of CO_2 flux. The varZc simulations modify the seasonal and annual means of CO_2 flux of SLD and depict it as a source of CO_2 especially during the monsoon, but the magnitude is still underestimated compared to Takahashi et al., (2009) observations. The SCTR variability is underestimated by both constZc and varZc simulations, portraying it as a CO_2 sink region whereas observations over the monsoon period indicate that the thermocline ridge driven by the open ocean wind-stress curl is in fact an oceanic source of CO_2. However, the varZc simulation reduced the magnitude of the sink in this region bringing it relatively closer to observations.

VarZc biological parameterization strengthens the export and new productions in the model, which allows it to a represent better seasonal cycle of CO_2 and pCO_2 over the study regions. The WAS export production is remarkably improved by 62.37 ± 7.8 g C m^{-2} yr^{-1} compared to constZc. This supports our conclusion that the varZc parameterization increases the strength of biological export in the model. Over the SLD, the JJAS seasonal mean export and new productions are underestimated in varZc compared to constZc simulations, but the annual mean

Biogeosciences Discuss., doi:10.5194/bg-2017-114, 2017
Manuscript under review for journal Biogeosciences
Discussion started: 28 April 2017

624 export production is improved. Export production at the SC and SCTR are highly exaggerated
625 and there is hardly any improvement in new production with a variable Zc especially over the
626 monsoon period. The inability of varZc parameterization to improve the seasonality of SC and
627 SCTR may be due to the interannnual variability of biological production associated with the
628 Indonesian throughflow and remote forcing of the mixed layer-thermocline interactions and the
629 effect of biases in the windstress data used as a physical driver in the model.

630 Further sensitivity experiments carried out with providing annual mean currents or
631 temperatures in selected subdomains reveal that the varZc retains the seasonality of carbon
632 fluxes, pCO_2, export and new productions in the right direction as in the observations. This
633 strongly supports our contention that varZc parameterization improves the export and new
634 productions and it is also efficient in capturing upwelling episodes of the study regions. This
635 points out the significant role of having a proper balance in seasonal biological export and new
636 production in models to capture the seasonality in carbon cycle. This also confirms the role of
637 biological and solubility pumps in producing the seasonality of carbon cycle in the upwelling
638 zones.

639 However the underestimation of seasonality of CO_2 flux over the SLD and overestimation
640 over the SC as well as the SCTR is a cautionary flag for the study. This uncertainty poses an
641 important scientific question as to whether the model biology over the SC and SCTR region is
642 not resolving the seasonality in CO_2 flux and pCO_2 properly or whether the seasonality in the
643 compensation depth is not able to fully capture the biological processes.

644 To address these questions we have used inverse modeling methods (Bayesian inversion) in
645 order to optimize the spatially and temporally varying compensation depth using surface pCO_2 as

Biogeosciences Discuss., doi:10.5194/bg-2017-114, 2017
Manuscript under review for journal Biogeosciences
Discussion started: 28 April 2017

646 the observational constraints and computed the optimized biological production. The results will
647 be reported elsewhere.

648

649

650

651

652

653

654

655

656

657

658

659

660

661

662

663

Biogeosciences Discuss., doi:10.5194/bg-2017-114, 2017
Manuscript under review for journal Biogeosciences
Discussion started: 28 April 2017

Appendix - A

For $Z < Z_c$,

$$J_{prod} = \frac{1}{\tau}([PO_4] - [PO_4^*]), \quad [PO_4] > [PO_4^*] \tag{A1}$$

$$J_{DOP} = \sigma J_{prod} - \kappa[DOP] \tag{A2}$$

$$J_{PO4} = -J_{prod} + \kappa[DOP] \tag{A3}$$

$$J_{ca} = Rr_{C:P}(1-\sigma)J_{prod} \tag{A4}$$

$$J_{DIC} = r_{C:P}J_{PO4} + J_{ca} \tag{A5}$$

$$J_{ALK} = -r_{N:P}J_{PO4} + 2J_{ca} \tag{A6}$$

For $Z > Z_c$,

$$J_{prod} = 0, \quad [PO_4] \leq [PO_4^*] \tag{A7}$$

$$J_{DOP} = -\kappa[DOP] \tag{A8}$$

$$J_{PO4} = -\frac{\partial F}{\partial Z} + \kappa[DOP] \tag{A9}$$

$$F(Z) = F_c\left(\frac{Z}{Zc}\right)^{-a} \tag{A10}$$

$$F_c = (1-\sigma)\int_0^{Zc} J_{prod}\, dZ \tag{A11}$$

$$J_{ca} = -\frac{\partial F_{Ca}}{\partial Z} \tag{A12}$$

$$F_{Ca} = Rr_{C:P}F_C e^{-(z-Zc)/d} \tag{A13}$$

Biogeosciences Discuss., doi:10.5194/bg-2017-114, 2017
Manuscript under review for journal Biogeosciences
Discussion started: 28 April 2017

Where Z is the depth and Z_c is the compensation depth in the model. J_{prod} , J_{DOP} , J_{PO4} , J_{Ca} are the biogeochemical sources and sinks. Within the compensation depth (Z_c), the biological production in the model J_{prod} is calculated using equation A1. $[PO_4]$ is the model phosphate concentration and $[PO_4^*]$ is observational phosphate. τ is the restoration timescale taken as 30 days. Whenever the model phosphate exceeds the observational phosphate, it allows production.The observational phosphate data were taken from the World Ocean Atlas (*WOA*) 1994 [*Conkright et al.,* 1994]. During the biological production a fixed fraction (σJ_{prod}) of phosphate is converted into Dissolved Organic Phosphate (DOP) which is a source for J_{DOP} [equation A2] and remaining $-\kappa[DOP]$ is exported downward below the compensation depth, which is further remineralized into inorganic phosphate and made available for further biological production [equation A3]. The downward flux of phosphate which is not converted into DOP within the compensation depth is given by equation A11. The decrease of flux with depth due to remineralization is shown by equation A10. The values of the constants a, κ, σ are 0.9, $(0.2\ \text{year})^{-1}$ to $(0.7\ \text{year})^{-1}$, 0.67, respectively. The rate of production is used to explain the formation of calcium carbonate cycle in the surface waters [equation A4] and its export is given by equation A12. Where R is the rain ratio, a constant molar ratio of exported particulate organic carbon to the exported calcium carbonate flux at compensation depth. The exponential decrease of calcium carbonate flux with scale depth d is given by equation A13. The biological source or biological sink of dissolved inorganic carbon (DIC) and alkalinity (ALK) is explained through equations A5 and A6, respectively. Where the values of rain ratio (R) is taken as 0.07 and the Redfield ratio, $r_{C:P} = 106$,$r_{N:P} = 16$ and scale depth d is chosen as 3500m.

Biogeosciences Discuss., doi:10.5194/bg-2017-114, 2017
Manuscript under review for journal Biogeosciences
Discussion started: 28 April 2017

Acknowledgement

The OCMIP-II routines were taken from (http://ocmip5.ipsl.jussieu.fr/OCMIP/). GFDL data for OTTM is taken from (http://data1.gfdl.noaa.gov/nomads/forms/assimilation.html).Takahashi data is taken from (http://www.ldeo.columbia.edu/res/pi/CO2/).The computations were carried out in High Performance Computing (HPC) of Ministry of Earth Sciences (MoES), IITM. Ms. Shikha Singh, Ms. Anju M (IITM) and Mr. Saran Rajendran (CUSAT) are thanked for initial helps and discussions.

References

Anderson, L. A., Sarminento. J. L.: Global ocean phosphate and oxygen simulations, Global Biogeochem. Cycles., 9, 621-636, doi:10.1029/95GB01902, 1995.

Asselin, R.: Frequency filter for time integrations, Mon. Wea. Rev., 100, 487–490, doi: 10.1175/1520-0493, 1972.

Banse, K.: Seasonality of phytoplankton chlorophyll in the central and northern Arabian Sea, Deep Sea Res., 34, 713 – 723, doi:10.1016/0198-0149, 1987.

Banse, K., McClain, C. R.: Winter blooms of phytoplankton in the Arabian Sea as observed by the Coastal Zone Color Scanner, Mar. Ecol. Prog. Ser., 34, 201 – 211, 1986.

Barber, R. T., Marra. J., Bidigare. R. C., Codispoti. L. A., Halpern. D., Johnson. Z., Latasa. M., Goericke. R., and Smith. S. L.: Primary productivity and its regulation in the Arabian Sea during 1995, Deep. Sea. Res, pt. II, 48, 1127 – 1172. doi:10.1016/S0967-0645, 2001.

Bates, N. R., Pequignet. A. C., and Sabine. C. L.: Ocean carbon cycling in the Indian Ocean: 2. Estimates of net community production, Global Biogeochem. Cycles., 20, GB3021, doi:10.1029/2005GB002492, 2006.

Bauer, S., Hitchcock, G. L., Olson, D. B.: Influence of monsoonally-forced Ekman dynamics upon surface-layer depth and plankton biomass distribution in the Arabian Sea, Deep Sea Res., 38, 531 – 553, doi:10.1016/0198-0149, 1991.

Behrenfeld, M. J., Falkowski. P. G.: Photosynthetic rates derived from satellite-based chlorophyll concentration, Limnol. Oceanogr., 42, 1 – 20, doi: 10.4319/lo.1997.42.1.0001, 1997.

741 Boyd, P. W., Rynearson, T. A., Armstrong, E. A., Fu. F., Hayashi. K. and co-authors.: Marine
742 Phytoplankton Temperature versus growth responses from polar to tropical waters – outcome of
743 a scientific community-wide study, PLoS ONE 8(5)., e63091,
744 Doi:10.1371/journal.phone.0063091, 2013.

745 Brock, J. C., McClain, C. R., Hay, W. W.: A southwest monsoon hydrographic climatology for
746 the northwestern Arabian Sea, J. geophys. Res., 97(C6), 9455 – 9465, doi: 10.1029/92JC00813,
747 1992.

748 Brock, J C., McClain, C. R.: Interannual variability of the southwest monsoon phytoplankton
749 bloom in the north-western Arabian Sea, J. geophys. Res., 97(C1), 733 – 750,
750 doi/10.1029/91JC02225, 1992.

751 Brock, J. C., McClain, C. R., Luther, M. E., Hay, W. W.: The phytoplankton bloom in the
752 northwestern Arabian Sea during the southwest monsoon of 1979, J. geophys. Res., 96(C11),
753 623 – 642, doi: 10.1029/91JC01711, 1991.

754 Brock. J., Sathyendranath. S., and Platt. T.: Modelling the seasonality of subsurface light and
755 primary production in the Arabian Sea, Mar. Eco. Prog. Ser., 101, 209 – 221, 1993.

756 Bruce, J. G.: Some details of upwelling off the Somali and Arabian coasts, J. mar. Res., 32, 419
757 – 423, 1974.

758 Bryan. K., Lewis, L. J.: A water mass model of the world ocean, J. Geophys. Res., 84, 2503 –
759 2517, doi: 10.1029/JC084iC05p02503, 1979.

760 Chang, Y. S., Zhang. S., Rosati. A., Delworth. T., Stern. W. F.: An assessment of oceanic
761 variability for 1960-2010 from the GFDL ensemble coupled data assimilation, Clim. Dyn., 40,
762 775 – 803, doi: 10.1007/s00382-012-1412-2, 2012.

763 Christian J. R., Verschall M. A., Murtugudde R., Busalacchi A. J., McClain C. R.:
764 Biogeochemical modelling of the tropical Pacific Ocean. II: Iron biogeochemistry, Deep Sea
765 Res., 49, 545 – 565, doi:10.1016/S0967-0645, 2001.

766 Colwell, R. R.: Global climate and infectious disease: the cholera paradigm, Science., 274(5295),
767 2025 – 2031, doi: 10.1126/science.274.5295.2025, 1996.

768 Dilmahamod A. F., Hermes. J. C., Reason C. J. C.: Chlorophyll-a variability in the Seychelles-
769 Chagos Thermocline Ridge: Analysis of a coupled biophysical model, J. of. Mar. Sys., 154, 220
770 – 232, doi:10.1016/j.jmarsys.2015.10.011, 2016.

771 Doney S. C., and co-authors.: Evaluating global ocean carbon models: The importance of
772 realistic physics, Glob. Biogeochem. Cycles., 18, doi:10.1029/2003GB002150, 2004.

773 Eppley, R. W.: Temperature and phytoplankton growth in the sea, Fish. Bull., 70, 1063 – 1085,
774 1972.

775 Eppley, R. W., Peterson. B. J.: Particulate organic matter flux and planktonic new production in
776 the deep ocean, Nature., 282, 677-680, doi:10.1038/282677a0, 1979.

777 Feely, R. A., Sabine, C. L., Takahashi, T., Wanninkhof, R.: Uptake and Storage of Carbon
778 Dioxide in the Ocean: The Global CO_2 Survey, Oceanography., 14(4), 18–32,
779 doi:10.5670/oceanog.2001.03, 2001.

780 Friedrichs, M. A. M., and co-authors.: Assessment of skill and portability in regional
781 biogeochemical models: role of multiple planktonic groups, J. GeoPhy. Res., 112, doi:
782 10.1029/2006JC003852, 2007.

783 Friedrichs, M. A. M., Hood, R. R., Wiggert, J. D.: Ecosystem complexity versus physical forcing
784 quantification of their relative impact with assimilated Arabian Sea data, Deep Sea Res., 53, 576-
785 600, doi:10.1016/j.dsr2.2006.01.026, 2006.

786 Garcia, H. E., R. A. Locarnini, T. P. Boyer, J. I. Antonov, O.K. Baranova, M.M. Zweng, J.R.
787 Reagan, D.R. Johnson.: World Ocean Atlas 2013, Volume 4: Dissolved Inorganic Nutrients
788 (phosphate, nitrate, silicate), S. Levitus, Ed., A. Mishonov Technical Ed.; NOAA Atlas NESDIS
789 76, 25 pp, 2014.

790 Gent, P. R., McWilliams. J. C.: Isopycnal mixing in ocean circulation models, J. Phys.
791 Oceanogr., 20, 150 – 155, doi: 10.1175/15200485, 1990.

792 Harwell, C., Kim, K., Burkholder, J., Colwell, R., Epstein, P. R., Grimes, D., Hofmann, E. E.,
793 Lipp, E. K., Osterhaus, A., and Overshreet, R. M.: Emerging marine diseases-climate links and
794 anthropogenic factors, Science., 285(5433), 1505 – 1510, doi: 10.1126/science.285.5433.1505,
795 1999.

796 Howden, S., Murtugudde, R.: Effects of river inputs into the Bay of Bengal, J. Geophys. Res.,
797 106, 19,825-19,843. doi: 10.1029/2000JC000656, 2001.

798 Jerlov N. G.: Marine optics, Second ed., Elsevier, pp 231, 1976.

799 Jung, E., and Kirtman. B. P.: ENSO modulation of tropical Indian ocean subseasonal variability,
800 Geophy. Res. Lett., 43, doi: 10.1002/2016GL071899, 2016.

Krey, J., Bahenerd, B.: Phytoplankton production atlas of the international Indian Ocean expedition, Institut fur Meereskundeander Universitat Kiel, Kiel, German.

Large, W. G., McWilliams, J. C., Doney, S. C.: Oceanic vertical mixing: A review and a model with a nonlocal boundary layer parameterization, Rev. Geophys., 32, 363 – 403, doi: 10.1029/94RG01872, 1994.

Le Quere, C., Orr, J. C., Monfray, P., Aumont, O.: Interannual variability of the oceanic sink of CO_2 from 1979 through 1997, Global Biogeochem. Cycles., 14, p1247 – 1265, doi: 10.1029/1999GB900049, 2000.

Lee, P. F., Chen, I. C., Tzeng. W. N.: Spatial and Temporal distributions patterns of bigeye tuna (Thunnusobsesus) in the Indian Ocean, Zoological studies-Taipei-, 44(2), 260, 2005.

Lehodey .P., Senina I., Sibert. J., Bopp. L., Calmettes B., Hampton .J., Murtugudde. R.: Preliminary forecasts of Pacific bigeye tuna population trends under the A2 IPCC scenario, Prog in Oceanography., 86, 302 – 315, doi:10.1016/j.pocean.2010.04.021, 2010.

Levy, M., Shankar, D., Andre, J. M., Shenoi, S., Durand, F., Montegut, C. B., 2007. Basin-wide seasonal evolution of the Indian Ocean's phytoplankton blooms, J. Geophy. Res. Oceans., 112(C12), 1978 – 2012, doi: 10.1029/2007JC004090, 2007.

Liao, X., Zhan, H., Du, Y.: Potential new production in two upwelling regions of the Western Arabian Sea: Estimation and comparison, J. Geophy. Res. Oceans., 121, doi:10.1002/2016JC011707, 2016.

Matsumoto K., Tokos. K. S., Price., A. R., Cox. S. J.: First description of the Minnesota Earth System Model for Ocean biogeochemistry (MESMO 1.0), Geosci. Model Dev., 1, 1-15, doi:10.5194/gmd-1-1-2008, 2008.

McCreary, J., Murtugude, R., Vialard, J., Vinayachandran, P., Wiggert, J. D., Hood, R. R., Shankar, D., Shetye, S.: Biophysical processes in the Indian Ocean, Indian Ocean Biogeochemical Processes and Ecological Variability., 9 – 32, doi: 10.1029/GM185, 2009.

Moisan, J. R., Moisan, A. T., Abbott, M. R.: Modelling the effect of temperature on the maximum growth rates of phytoplankton populations, Eco. Modelling., 153, 197-215, doi:10.1016/S0304-3800(02)00008, 2002.

Morel, A.: Optical modeling of the upper ocean in relation to its biogenous matter content (Case 1 Waters), J. Geophys. Res., 93, 10479-10, 768, doi: 10.1029/JC093iC09p10749, 1988.

Murtugudde R., McCreary J. P., Busalacchi, A. J.: Oceanic processes associated with anomalous events in the Indian Ocean with relevance to 1997-1998, J. Geophy. Res., 105, 3295-3306, doi: 10.1029/1999JC900294, 2000.

Murtugudde, R., Busalacchi, A. J.: Interannual variability of the dynamics and thermodynamics of the tropical Indian Ocean, J. Clim. 12, 2300-2326, doi:10.1175/1520-0442, 1999.

Murtugudde, R., Seager, R., Thoppil, P.: Arabian Sea response to monsoon variations, Paleoceanography., 22, PA4217, doi:10.1029/2007PA001467, 2007.

Najjar, R. G., Orr, J. C.: Design of OCMIP-2 simulations of chlorofluorocarbons, the solubility pump and common biogeochemistry, http://www.ipsl.jussieu.fr/OCMIP/., 1998.

840 Najjar, R. G., Keeling, R. F.: Analysis of the mean annual cycle of the dissolved oxygen
841 anomaly in the world ocean, J. Mar. Res., 55, 117 – 151, doi:10.1357/0022240973224481, 1997.

842 Najjar, R. G., Sarmiento, J. L., Toggweiler, J. R.: Downward transport and fate of organic matter
843 in the ocean: simulations with a general circulation model, Global biogeochem. Cycles., 6, 45-
844 76, doi/10.1029/91GB02718, 1992.

845 Naqvi, S. W. A., Moffett, J. W., Gauns, M. U., Narvekar, P. V., Pratihary, A. K., Naik, H.,
846 Shenoy, D. M., Jayakumar, D. A., Goepfert, T. J., Patra, P. K., Al-Azri, A., and Ahmed, S. I.:
847 The Arabian Sea as a high-nutrient, low-chlorophyll region during the late Southwest Monsoon,
848 Biogeosciences., 7, 2091-2100, doi:10.5194/bg-7-2091-2010, 2010.

849 Naqvi, S., Naik, H., Narvekar, P.: The Arabian Sea, in Biogeochemistry, edited by K. Black and
850 G. Shimmield, pp. 156 – 206, Blackwell, Oxford, 2003.

851 Orr, J. C., Aumont, O., Bopp, L., Calderia, K., Taylor, K., et. al.: Evaluation of seasonal air-sea
852 CO2 fluxes in the global carbon cycle models, International open Science conference (Paris, 7-
853 10 Jan. 2003), 2003.

854 Orr, J. C. and co-authors.: Estimates of anthropogenic carbon uptake from four three-
855 dimensional global ocean models, Glob. Biogeochem. Cycles., 15, p43 – 60, doi:
856 10.1029/2000GB001273, 2001.

857 Osawa, T., Julimantoro, S.: Study of fishery ground around Indonesia archipelago using remote
858 sensing data, International archives of the Photogrammetry, Remote sensing and spatial
859 information science., vol XXXVIII, part-8, 2010.

Parsons, T. R., Takahashi, M., Habgrave, B.: In Biological Oceanographic Processes, 3rd ed., 330pp., Pergamon Press, New York, doi: 10.1002/iroh.19890740411, 1984.

Prasanna Kumar, .S., Muraleedharan, P. M., Prasad, T. G., Gauns, M., Ramaiah, N., de Souza, S. N., Sardesai, S., Madhupratap, M.: Why is the Bay of Bengal less productive during summer monsoon compared to the Arabian Sea?, Geophys. Res. Lett., 29(24), 2235, doi:10.1029/2002GL016013, 2002.

Prasanna Kumar, S., Roshin, P. R., Narvekar, J., Dinesh Kumar, P., Vivekanandan, E.: What drives the increased phytoplankton biomass in the Arabian Sea?, Current Science, 99(I), 101 – 106, 2010.

Prassana Kumar. S, Ramaiah. N, Gauns. M., Sarma V. V. S. S., Muraleedharan. P. M., RaghuKumar. S., Dileep Kumar., Madhupratap. M.: Physical forcing of biological productivity in the Northern Arabian Sea during the Northeast Monsoon, Deep Sea Res. Pt. II., 48, 1115-1126, doi:10.1016/S0967-0645(00)00133-8, 2001.

Praveen, V., Ajayamohan, R. S., Valsala, V., Sandeep, S.: Intensification of upwelling along Oman coast in a warming scenario, Geophys. Res. Lett., 43, doi:10.1002/2016GL069638, 2016.

Qasim, S. Z.: Biological productivity of the Indian Ocean, J. mar. Sci., 6, 122 – 137, 1977.

Qasim, S. Z.: Oceanography of Northern Arabian Sea, Deep Sea Res., 29(9A), 1041 – 1068, doi:10.1016/0198-0149(82)90027-9, 1982.

Redi, M.: Oceanic isopycnal mixing by coordinate rotation, J. Phys. Oceanogr., 12, 1154 – 1158, doi: 10.1175/1520-0485, 1982.

880 Roxy, M. K., Modi, A., Murtugudde, R., Valsala, V., Panickal, S., Prasanna Kumar, S.,
881 Ravichandran, M., Vichi, M., Levy, M.: A reduction in marine primary productivity driven by
882 rapid warming over the tropical Indian Ocean, 43, 826 – 833, J. Geophy. Res. Letters.,
883 doi:10.1002/2015GL066979, 2015.

884 Ryther, J.: Photosynthesis in the ocean as function of light Intensity, Limnol. Oceanogr., vol 1,
885 issue 1, doi: 10.4319/lo.1956.1.1.0061, 2003.

886 Ryther, J., Menzel, D.: On the production, composition, and distribution of organic matter in the
887 Western Arabian Sea, Deep Sea Research and Oceanographic Abstracts., 12(2), 199 -209.
888 doi:10.1016/0011-7471(65)90025-2, 1965.

889 Sarma V. V. S. S.: Net plankton community production in the Arabian Sea based on O_2 mass
890 balance model, Glob. biogeochem. Cycles., 18, GB4001, doi:10.1029/2003GB002198, 2004.

891 Sarma, V. V. S. S.: An evaluation of physical and biogeochemical processes regulating the
892 perennial suboxic conditions in the water column of the Arabian Sea, Global Biogeochem.
893 Cycles., 16, doi:10.1029/2001GB001461, 2002.

894 Sarmiento, J. L., and Gruber, N.: Ocean Biogeochemical Dynamics, Princeton University Press,
895 New Jersey, 2006.

896 Sarmiento, J. L., Monfray. P., Maier-Reimer., Aumont, O., Murnane, R. J., Orr, J. C.: Sea-air
897 CO_2 fluxes and carbon transport: A comparison of three ocean general circulation models,
898 Global Biogeochem. Cycles., 14, p1267 – 1281. doi: 10.1029/1999GB900062, 2000.

899 Schott, F.: Monsoon response of the Somali current and associated upwelling, Prog.Oceanogr.,
900 12, 357 – 381, doi:10.1016/0079-6611(83)90014-9, 1983.

Smetacek, V., and Passow, U.: Spring bloom initiation and Sverdrup's critical depth model, Limnol. Oceanogr., 35, 228 – 234, doi: 10.4319/lo.1990.35.1.0228, 1990.

Smith, L. S.: Understanding the Arabian Sea: Reflections on the 1994-1996 Arabian Sea Expedition, Deep Sea Res. Pt. II., 48, 1385-1402, doi:10.1016/S0967-0645(00)00144-2, 2001.

Smith, R. L., Bottero, L. S.: On upwelling in the Arabian Sea. In Angel, M (ed) A voyage of Discovery. Pergammon Press, New York, p. 291 – 304, 1977.

Smith, S. L.: Biological indications of active upwelling in the northwestern Indian Ocean in 1964 and 1979, a comparison with peru and northwest Africa, Deep Sea Res., 31, 951 – 967, doi:10.1016/0198-0149(84)90050-5, 1984.

Smith, S. L., Codistpoti, L. A.: Southwest monsoon of 1979: chemical and biological response of Somali coastal waters. Science, 209, 597 – 600. doi:10.1126/science.209.4456.597, 1980.

Susanto. R., Gordon, A. L., Zheng. Q.: Upwelling along the coasts of Java and Sumatra and its relation to ENSO, J. Geophy. Res. Lett., 28, 1599-1602, doi: 10.1029/2000GL011844, 2001.

Swallow, J. C.: Some aspects of the physical oceanography of the Indian Ocean, Deep Sea Res., 31, 639 – 650, doi:10.1016/0198-0149(84)90032-3, 1984.

Takahashi, T., Sutherland, S. C., Wanninkhof, R., Sweeney, C., Feely, R. A., Chipman, D. W., Hales, B., Friederich, G., Chavez, F., Sabine, C., et al.: Climatological mean and decadal changes in surface ocean pCO_2 and net sea-air CO_2 flux over the global oceans. Deep Sea Res., Pt. II., 56, 554 – 557, doi:10.1016/j.dsr2.2008.12.009, 2009.

Valsala V., Maksyutov, S.: Interannual variability of air-sea CO_2 flux in the north Indian Ocean, Ocean Dynamics., 1 – 14, doi 10.1007/s10236-012-0588-7, 2013.

922 Valsala, K. V., Maksyutov, S., Ikeda, M.: Design and Validation of an offline oceanic tracer
923 transport model for a carbon cycle study, J. clim., 21, doi: 10.1175/2007JCLI2018.1, 2008.

924 Valsala, V., Murtugudde, R.: Mesoscale and Intraseasonal Air-Sea CO_2 Exchanges in the
925 Western Arabian Sea during Boreal Summer, Deep Sea Res. Pt. I, 103, 103-113,
926 doi:10.1016/j.dsr.2015.06.001, 2015.

927 Valsala, V., Roxy, M., Ashok, K., Murtugudde, R.: Spatio-temporal characteristics of seasonal to
928 multidecadal variability of pCO_2 and air-sea CO_2 fluxes in the equatorial Pacific Ocean, J.
929 Geophys. Res., 119, 8987 – 9012, doi:10.1002/2014JC010212, 2014.

930 Valsala, V., Maksyutov, S., Murtugudde, R.: Interannual to Interdecadal Variabilities of the
931 Indonesian Throughflow Source Water Pathways in the Pacific Ocean, J. Phys. Oceanogr., 41,
932 1921–1940, doi: 10.1175/2011JPO4561.1, 2011.

933 Valsala, V., Maksyutov, S.: Simulation and assimilation of global **oc**ean pCO_2 and air-sea CO_2
934 fluxes using ship observations of surface ocean pCO_2 in a simplified biogeochemical model,
935 Tellus., 62B, doi: 10.1111/j.1600-0889.2010.00495, 2010.

936 Vialard,. J. P. and co-authors.: Air-Sea Interactions in the Seychelles-Chagos Thermocline Ridge
937 Region, BAMS, doi:10.1175/2008BAMS2499.1, 2009.

938 Vinayachandran P. N., Yamagata, T.: Monsoon Response of the Sea around Sri Lanka:
939 Generation of Thermal Domes and Anticyclonic Vortices, J. Phy. Oceano., 28, 1946 – 1960, doi:
940 10.1175/1520-0485, 1998.

941 Vinayachandran P. N., Shankar D., S. Vernekar, K. K. Sandeep, P. Amol, C. P. Neema and A.
942 Chatterjee.: A summer monsoon pump to keep the bay of Bengal salty, Geophys. Res. Lett., 40,
943 1777 – 1782, doi:10.1002/grl.50274, 2013.

944 Vinayachandran, P. N., Mathew, S.: Phytoplankton bloom in the Bay of Bengal during the
945 northeast monsoon and its intensification by cyclones, Geophy. Res. Lett., 30(11), 1572,
946 doi:10.1029/2002GL016717, 2003.

947 Vinayachandran, P. N., Chauhan, P., Mohan, M., Nayak, S.: Biological response of the sea
948 around Sri Lanka to summer monsoon, Geophys. Res. Lett., 31, L0I302,
949 doi:10.1029/2003GL018533, 2004.

950 Wang .X. J., Behrenfeld. M., Le Borgne .R., Murtugudde .R., and Boss. E.: Regulation of
951 phytoplankton carbon to chlorophyll ratio by light, nutrients and temperature in the equatorial
952 Pacific Ocean: a basin-scale model. Biogeosciences., 6, 391 – 404, doi:10.5194/bg-6-391-2009,
953 2009.

954 Wiggert J. D., Jones. B. H., Dickey .T D., Brink .K. H., Weller .R .A., Marra. J., Codispoti. L.
955 A.: The Northeast Monsoon's impact on mixing, phytoplankton biomass and nutrient cycling in
956 the Arabian Sea, Deep Sea Res. Pt. II, 47, 1353-1385, doi:10.1016/S0967-0645(99)00147-2,
957 2000.

958 Wiggert, J. D., Hood, R. R., Banse, K., Kindle, J. C.: Monsoon-driven biogeochemical processes
959 in the Arabian Sea, Progr. Oceanogr., 65, 176-213, doi:10.1016/j.pocean.2005.03.008, 2005.

960 Wiggert. J. D., Murtugudde, R. G., Christian J. R.: Annual ecosystem variability in the tropical
961 Indian Ocean: results of a coupled bio-physical ocean general circulation model, Deep Sea Res.
962 Pt. II., 53, 644-676, doi:10.1016/j.dsr2.2006.01.027, 2006.

963 Xie, S. P., Annamalai, H., Schott, F. A., McCreary Jr. J. P.: Structure and mechanism of south
964 Indian ocean climate variability, J. clim., 15, 864 – 878, doi: 10.1175/1520-0442, 2002.

965 Xing W., Xiaomei. L., Haigang Z., Hailong. L.: Estimates of potential new production in the
966 Java-Sumatra upwelling system, Chinese Journal of Oceanology and Limnology., 30, 1063-
967 1067, doi:10.1007/s00343-012-1281, 2012.

968 Yamanaka, Y., Yoshie, N, MasahikoFujii, Maka .N. Aita and Kishi. M. J.: An Ecosystem
969 coupled with Nitrogen-Silicon-Carbon cycles applied to station A7 in the Northwestern Pacific,
970 J. of Oceanogr., 60, p227-241, doi: 10.1023/B:JOCE.0000038329.91976.7d, 2004.

971 Zhou X., Weng. E., Luo., Y.: Modelling patterns of nonlinearity in the ecosystem responses to
972 temperature, CO_2 and precipitation changes, Eco. Appli., 18, 453 – 466, doi: 10.1890/07-0626.1,
973 2008.

974

Biogeosciences Discuss., doi:10.5194/bg-2017-114, 2017
Manuscript under review for journal Biogeosciences
Discussion started: 28 April 2017

Table: 1 WAS = Western Arabian Sea, SLD = Sri Lanka Dome, SC = Sumatra Coast, SCTR = Seychelles-Chagos Thermocline Ridge. JJAS mean and Climatological annual mean of CO_2 flux from Takahashi observations, constZc and varZc simulations. Units are in mol m^{-2} yr^{-1}.

Regions	CO_2 flux (mol m^{-2} yr^{-1})					
	JJAS Mean			Annual Mean		
	OBS	constZc	varZc	OBS	constZc	varZc
WAS	1.99	1.44 ± 0.2	2.31 ± 0.4	0.94	0.80 ± 0.1	1.07 ± 0.2
SLD	1.79	-0.008 ± 0.2	0.24 ± 0.09	0.80	-0.02 ± 0.1	0.10 ± 0.2
SC	0.31	0.60 ± 0.5	1.51 ± 1.01	0.21	0.21 ± 0.3	0.53 ± 0.5
SCTR	0.82	-0.32 ± 0.3	-0.05 ± 0.4	0.55	-0.02 ± 0.1	-0.07 ± 0.2

Table: 2 Same as Table 1, but for pCO_2. Units are in µatm.

Regions	pCO_2 (µatm)					
	JJAS Mean			Annual Mean		
	OBS	constZc	varZc	OBS	constZc	varZc
WAS	397.58	389.18 ± 3.7	399.95 ± 5.01	394.69	389.62 ± 3.9	391.19 ± 4.7
SLD	382.44	371.67 ± 6.04	379.24 ± 8.9	380.21	370.76 ± 6.1	374.94 ± 9.6
SC	372.52	382.36 ± 12.7	402.14 ± 21.8	372.69	374.65 ± 9.3	381.76 ± 13.6
SCTR	377.18	365.71 ± 5.08	370.72 ± 7.4	379.89	372.69 ± 4.7	369.00 ± 5.4

Biogeosciences Discuss., doi:10.5194/bg-2017-114, 2017
Manuscript under review for journal Biogeosciences
Discussion started: 28 April 2017

Table: 3 JJAS mean and Climatological annual mean of Export production from satellite derived Net Primary Production data, constZc and varZc simulations. Units are in g C m^{-2} yr^{-1}.

Regions	Export Production (g C m^{-2} yr^{-1})					
	JJAS Mean			Annual Mean		
	OBS	constZc	varZc	OBS	constZc	varZc
WAS	123.57	84.81 ± 16.04	147.19 ± 23.8	94.31	77.41 ± 15.1	122.54 ± 25.2
SLD	51.54	167.71 ± 59.04	151.51 ± 46.4	43.25	144.43 ± 49.8	156.08 ± 43.8
SC	58.87	260.11 ± 104.7	310.03 ± 99.5	54.53	172.52 ± 72.4	215.52 ± 70.8
SCTR	51.08	57.39 ± 14.2	99.23 ± 21.8	40.45	55.15 ± 17.9	80.35 ± 26.04

Table: 4 Same as Table 3, but for New production.

Regions	New Production (g C m^{-2} yr^{-1})					
	JJAS Mean			Annual Mean		
	OBS	constZc	varZc	OBS	constZc	varZc
WAS	--	150.84 ± 27.9	133.03 ± 19.5	--	108.43 ± 23.4	81.47 ± 15.7
SLD	--	141.93 ± 64.1	77.78 ± 27.6	--	111.05 ± 71.1	50.37 ± 26.3
SC	--	63.64 ± 30.9	78.11 ± 29.1	--	56.69 ± 43.3	54.58 ± 23.3
SCTR	--	12.17 ± 16.3	13.32 ± 18.6	--	13.74 ± 15.5	12.94 ± 13

Biogeosciences Discuss., doi:10.5194/bg-2017-114, 2017
Manuscript under review for journal Biogeosciences
Discussion started: 28 April 2017

Table 5: Table shows JJAS mean and climatological annual mean response from the model forced with annual mean currents.

WAS region forced with Annual mean currents	JJAS mean		Improvement	Climatological Annual mean		Improvement
	constZc	varZc		constZc	varZc	
CO_2 flux (mol m^{-2} yr^{-1})	0.80 ± 0.2	1.29 ± 0.2	0.48 ± 0.04	0.65 ± 0.1	0.79 ± 0.1	0.13 ± 0.02
pCO_2 (µatm)	381.81 ± 3.4	387.24 ± 3.9	5.43 ± 0.5	388.68 ± 3.4	388.40 ± 3.6	-0.28 ± 0.1
Export production (g C m^{-2} yr^{-1})	60.71 ± 4.7	104.22 ± 13.4	43.51 ± 8.6	74.30 ± 4.5	104.58 ± 18.3	30.28 ± 13.7
New Production (g C m^{-2} yr^{-1})	34.76 ± 2.3	52.16 ± 1.51	17.39 ± 0.8	29.91 ± 1.7	44.72 ± 1.6	14.81 ± 0.1

Table 6 Same as Table 5 but from annual mean temperature simulations.

WAS region forced with Annual mean temperature	JJAS mean		Improvement	Climatological Annual mean		Improvement
	constZc	varZc		constZc	varZc	
CO_2 flux (mol m^{-2} yr^{-1})	1.85 ± 0.2	2.74 ± 0.4	0.88 ± 0.1	0.81 ± 0.1	1.10 ± 0.2	0.28 ± 0.07
pCO_2 (µatm)	393.20 ± 3.01	404.26 ± 4.9	11.05 ± 1.9	384.61 ± 3.3	386.52 ± 4.8	1.91 ± 1.4

Biogeosciences Discuss., doi:10.5194/bg-2017-114, 2017
Manuscript under review for journal Biogeosciences
Discussion started: 28 April 2017

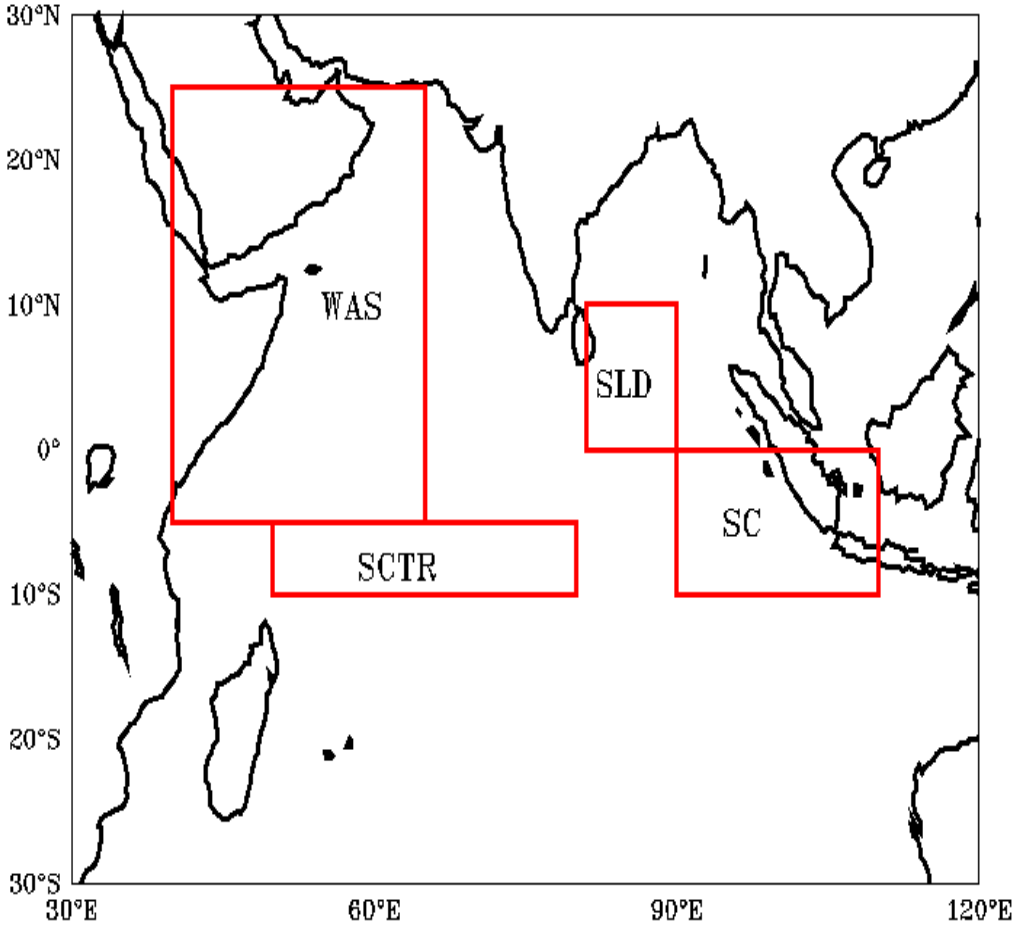

Fig (1) Red boxes shows the study regions (1) WAS (Western Arabian Sea, [40°E:65°E, 5°S:25°N]) (2) SLD (Srilankan Dome, [81°E:90°E, 0°:10°N]) (3) SCTR (Seychelles-Chagos Thermocline Ridge, [50°E:80°E, 5°S:10°S]) (4) SC (Sumatra Coast, [90°E:110°E, 0°:10°S]).

Biogeosciences Discuss., doi:10.5194/bg-2017-114, 2017
Manuscript under review for journal Biogeosciences
Discussion started: 28 April 2017

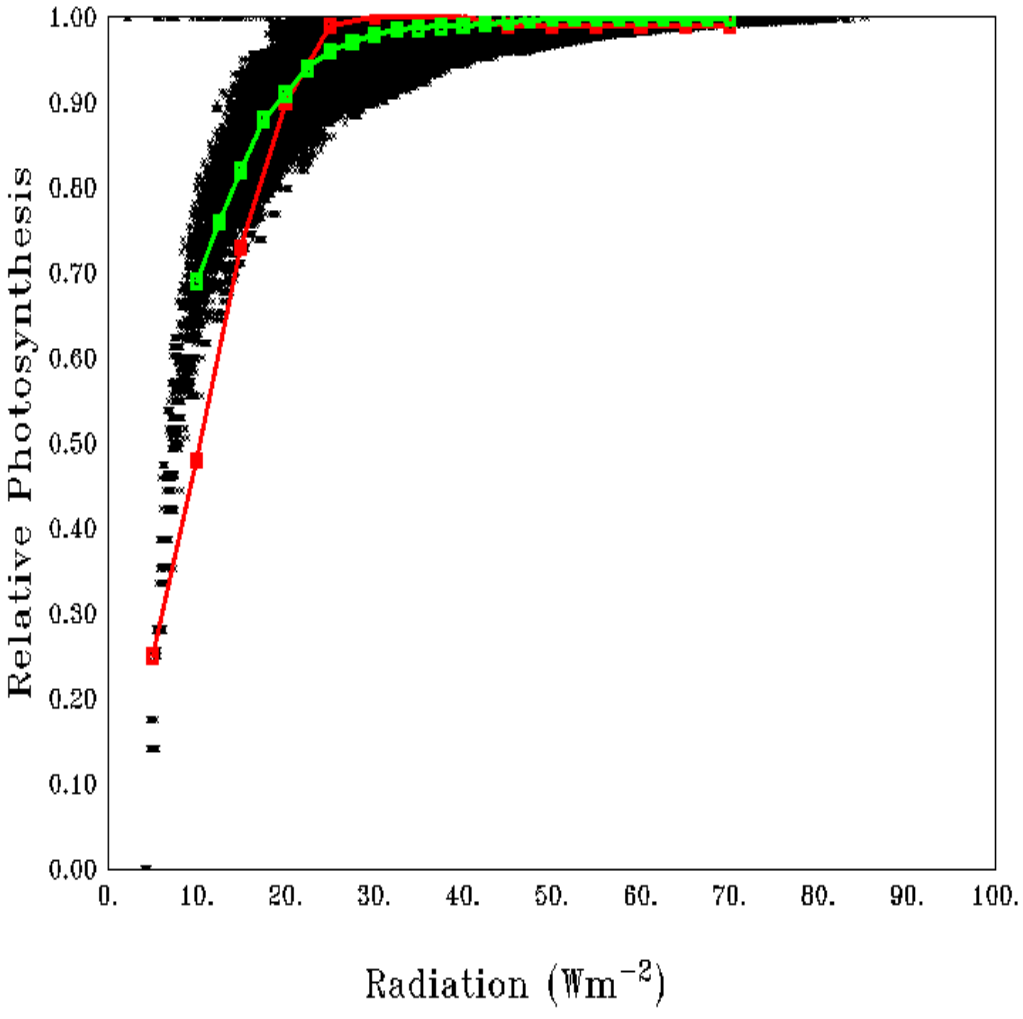

Fig (2) P – I curve, Scatter for average relative photosynthesis against different light intensities in the model. Red curve shows the theoretical P – I curve from Parsons et al., (1984). Green curve shows average of the scatter in the model.

Biogeosciences Discuss., doi:10.5194/bg-2017-114, 2017
Manuscript under review for journal Biogeosciences
Discussion started: 28 April 2017

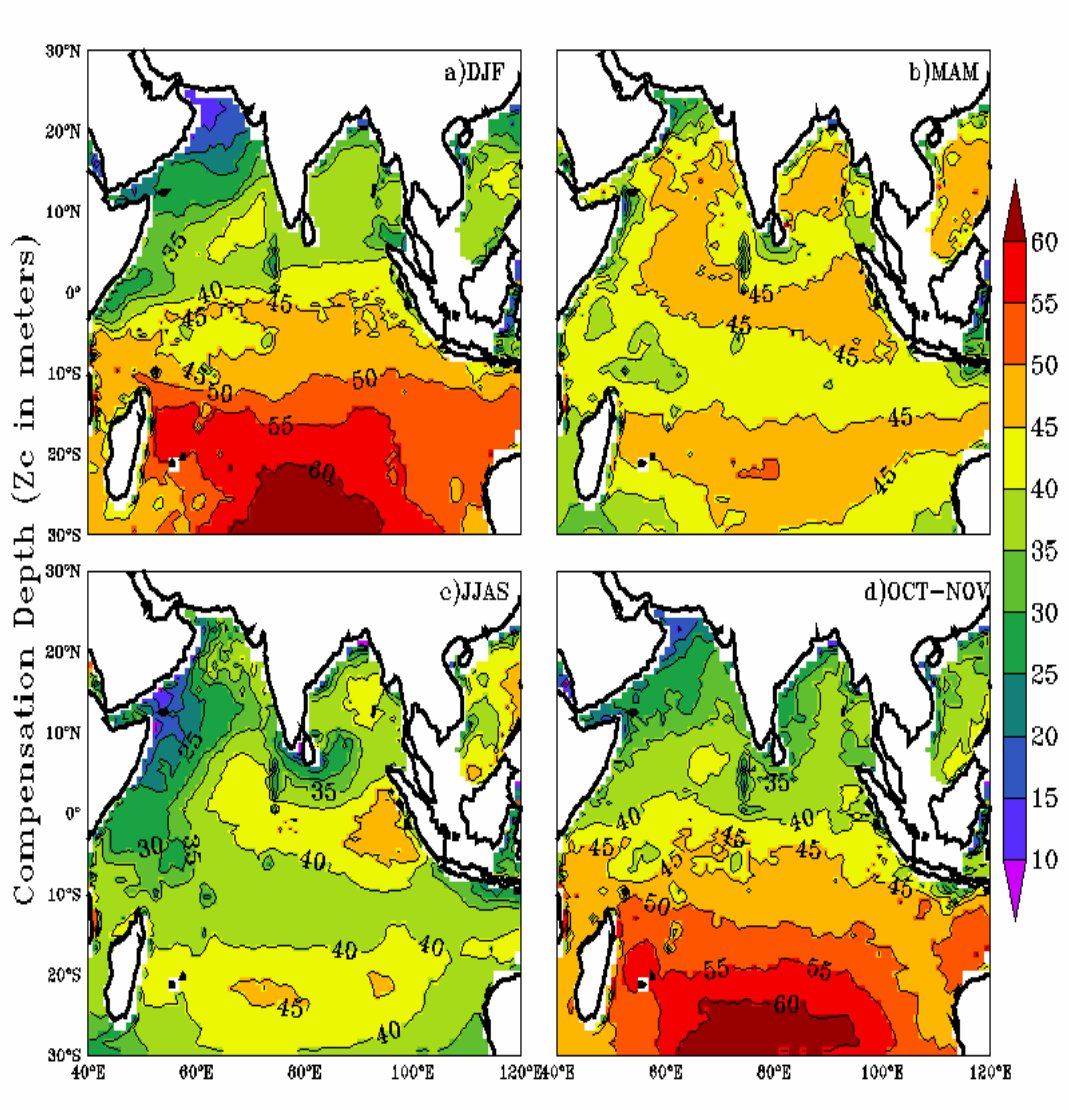

Fig (3): Seasonal mean map of Compensation Depth (Zc) as a function of Chl-a and light (a) DJF, (b) MAM, (c) JJAS, (d) OCT-NOV. Units are in meters.

Biogeosciences Discuss., doi:10.5194/bg-2017-114, 2017
Manuscript under review for journal Biogeosciences
Discussion started: 28 April 2017

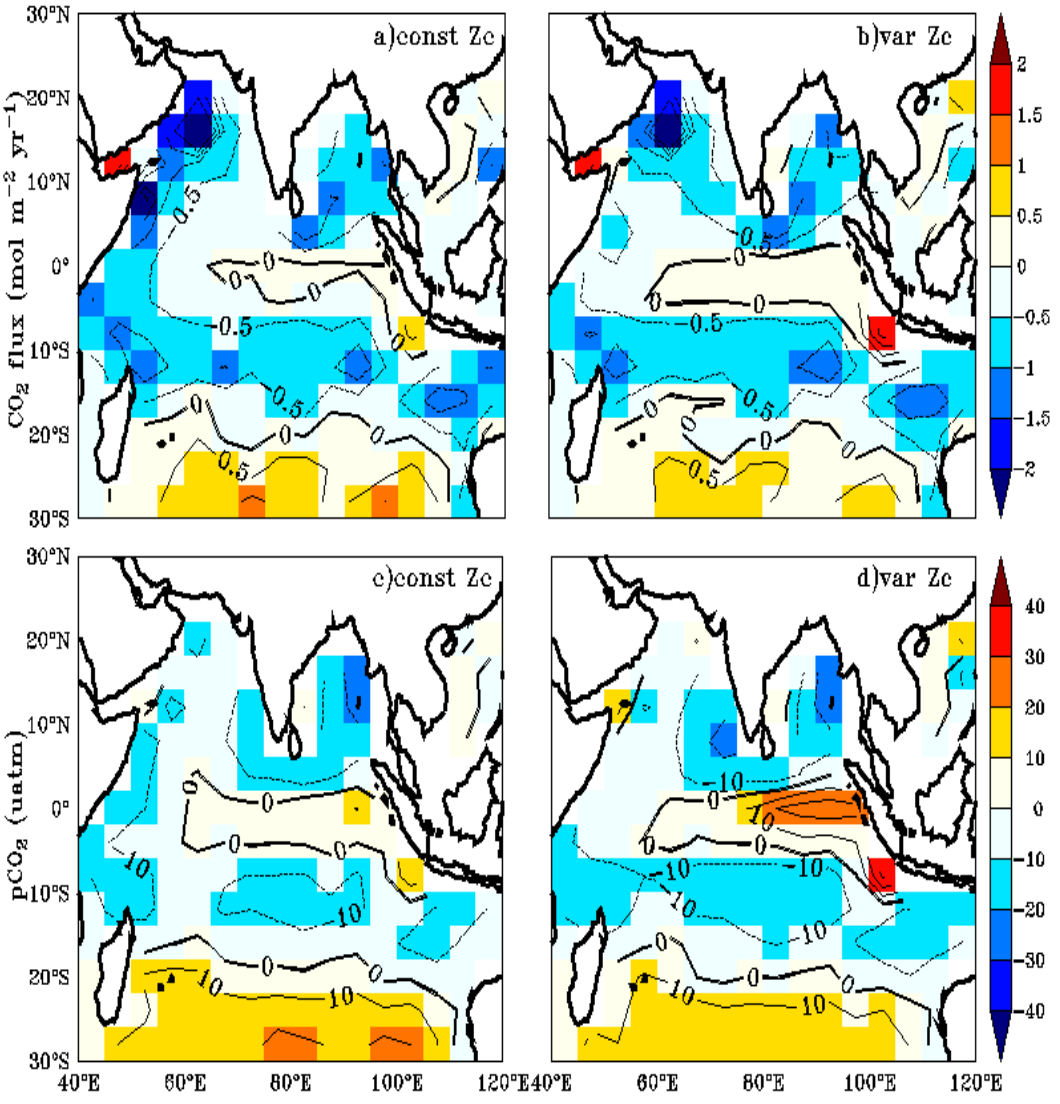

Fig (4): Annual mean biases in model evaluated against Takahashi observations for CO_2 flux (a,b) and pCO_2 (c, d) with constant Zc (constZc) and Varying Zc (varZc). Units of CO_2 flux and pCO_2 are mol m^{-2} yr^{-1} and µatm respectively.

Biogeosciences Discuss., doi:10.5194/bg-2017-114, 2017
Manuscript under review for journal Biogeosciences
Discussion started: 28 April 2017

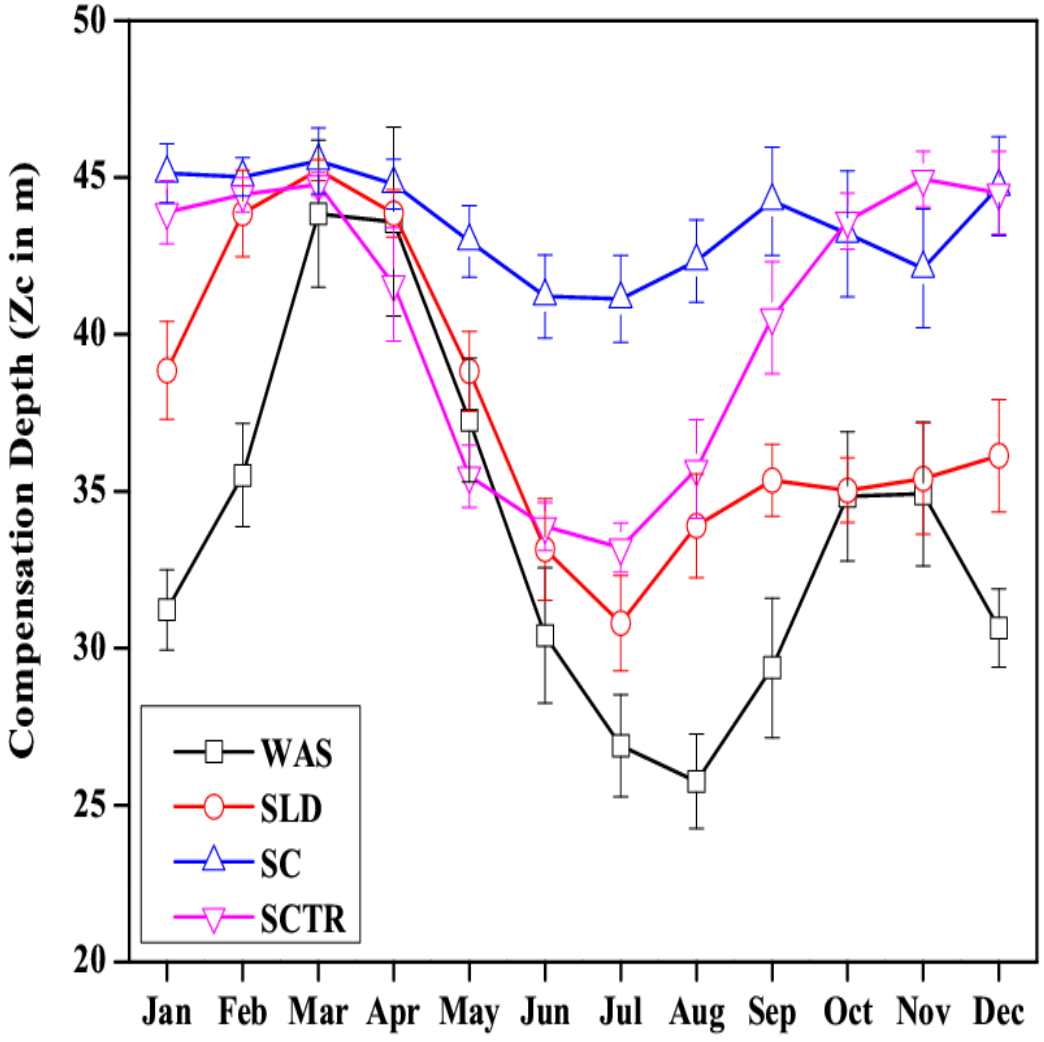

Fig (5): Seasonal variations in compensation depth (Zc) over the study regions as climatological state computed over 1990-2010. Error bar shows standard deviations of individual months over these years. Units are in meters.

Biogeosciences Discuss., doi:10.5194/bg-2017-114, 2017
Manuscript under review for journal Biogeosciences
Discussion started: 28 April 2017

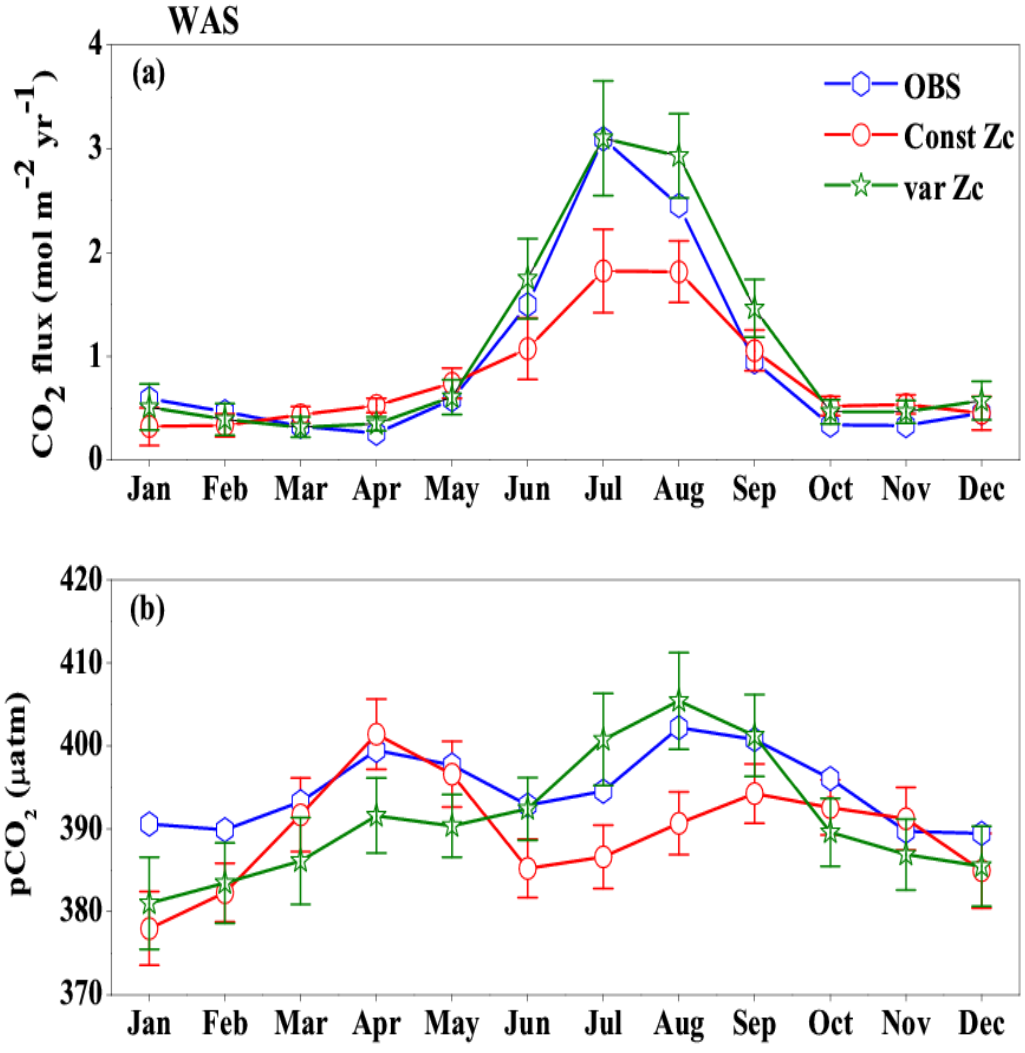

Fig (6): Comparison of model (a) CO_2 flux and (b) pCO_2 simulated with constant Zc (const Zc) and varying Zc (var Zc) with Takahashi Observations (OBS) over Western Arabian Sea (WAS) region as climatological state computed over 1990-2010. Error bar shows standard deviations of individual months over these years. Units of CO_2 flux and pCO_2 are mol m^{-2} yr^{-1} and µatm respectively. Legend is common for both graphs.

Biogeosciences Discuss., doi:10.5194/bg-2017-114, 2017
Manuscript under review for journal Biogeosciences
Discussion started: 28 April 2017

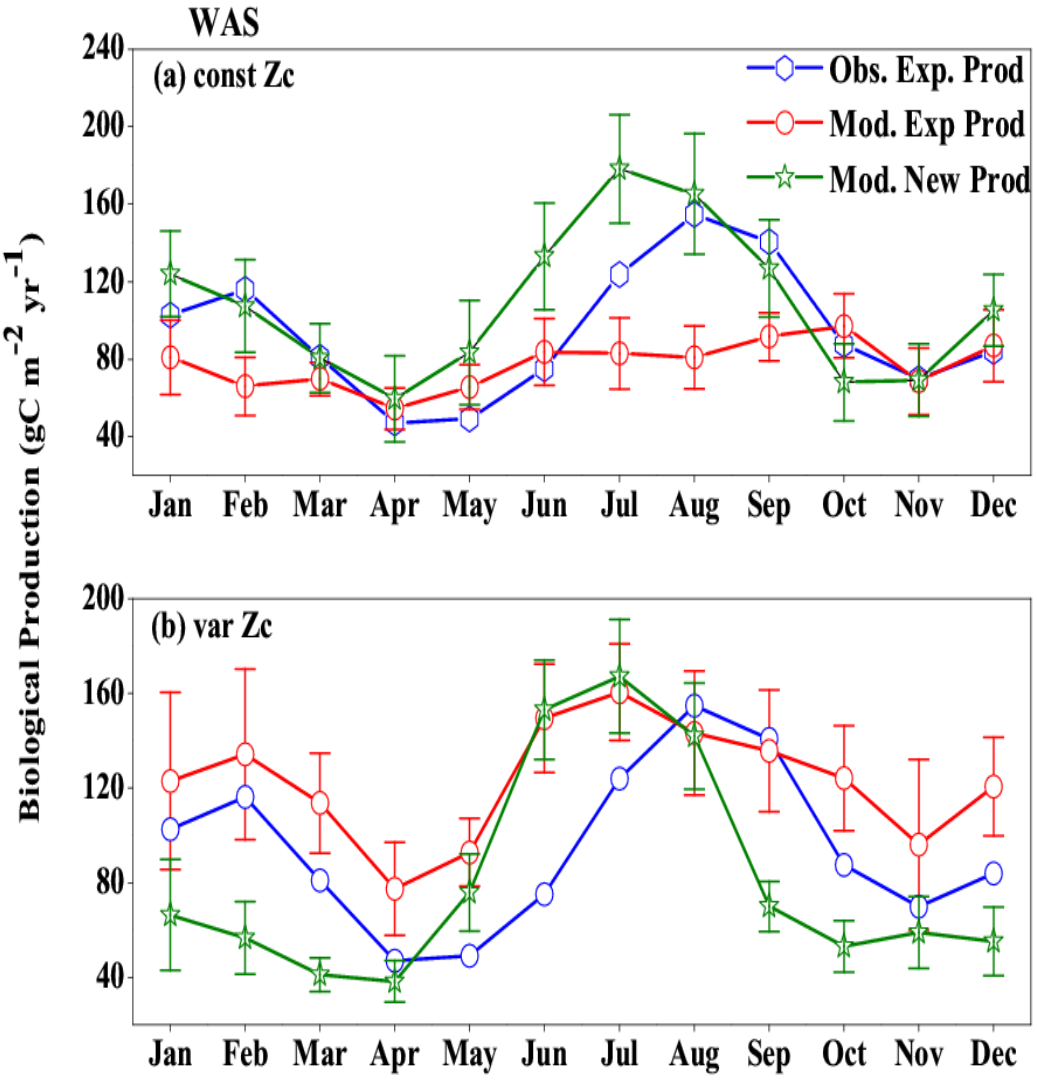

Fig (7): Comparison of model export production (Mod. Exp. Prod) and New production (Mod. New Prod) with satellite derived export production (Obs. Exp. Prod) for (a) Const Zc and (b) var Zc simulations for Western Arabian Sea (WAS) region. Units are in g C m^{-2} yr^{-1}. Legends are common for both graphs.

Biogeosciences Discuss., doi:10.5194/bg-2017-114, 2017
Manuscript under review for journal Biogeosciences
Discussion started: 28 April 2017

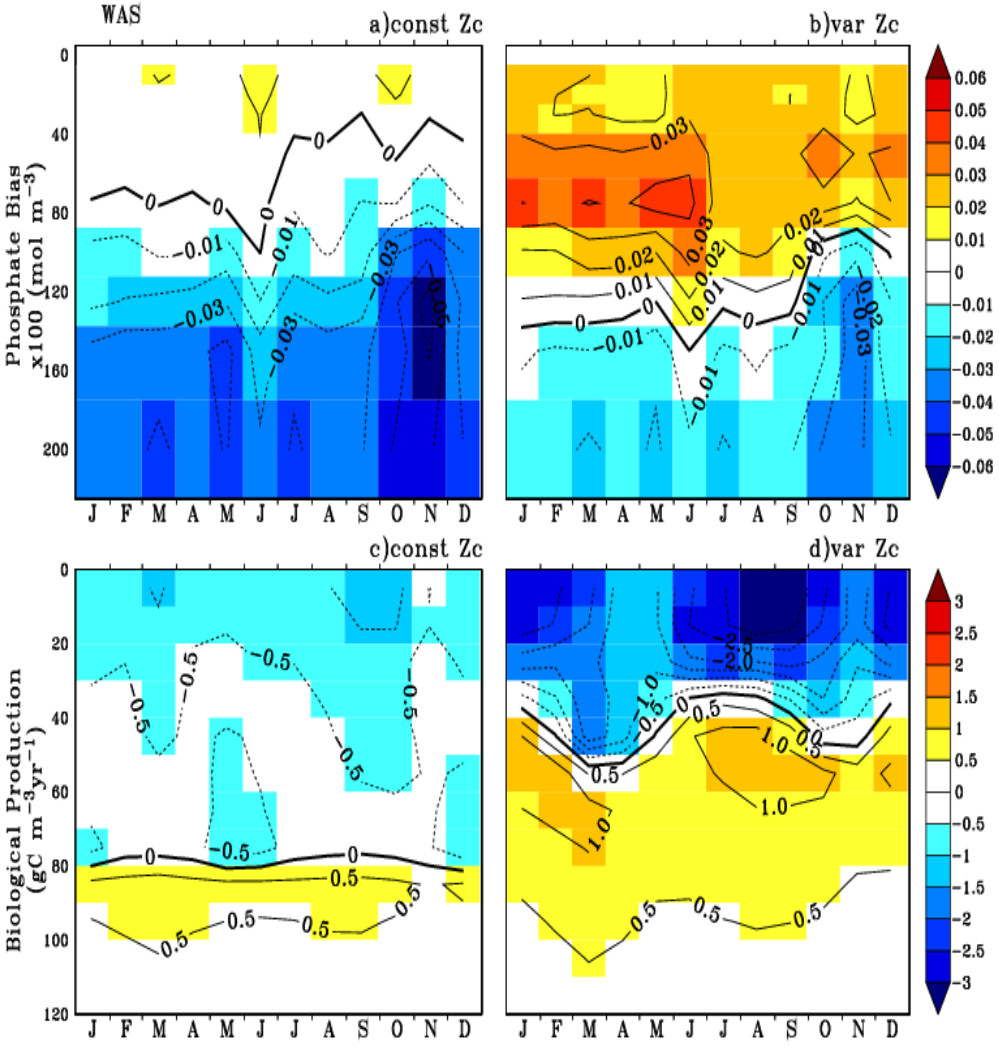

Fig (8): Bias estimation of Phosphate in the model with climatological observational data (a) const Zc and (b) Var Zc simulations and corresponding Biological production (c, d) in the model for Western Arabian Sea (WAS) region. Units of Phosphate (x 100 mol m^{-3}) and Biological Production (g C m^{-3} yr^{-1}).

Biogeosciences Discuss., doi:10.5194/bg-2017-114, 2017
Manuscript under review for journal Biogeosciences
Discussion started: 28 April 2017

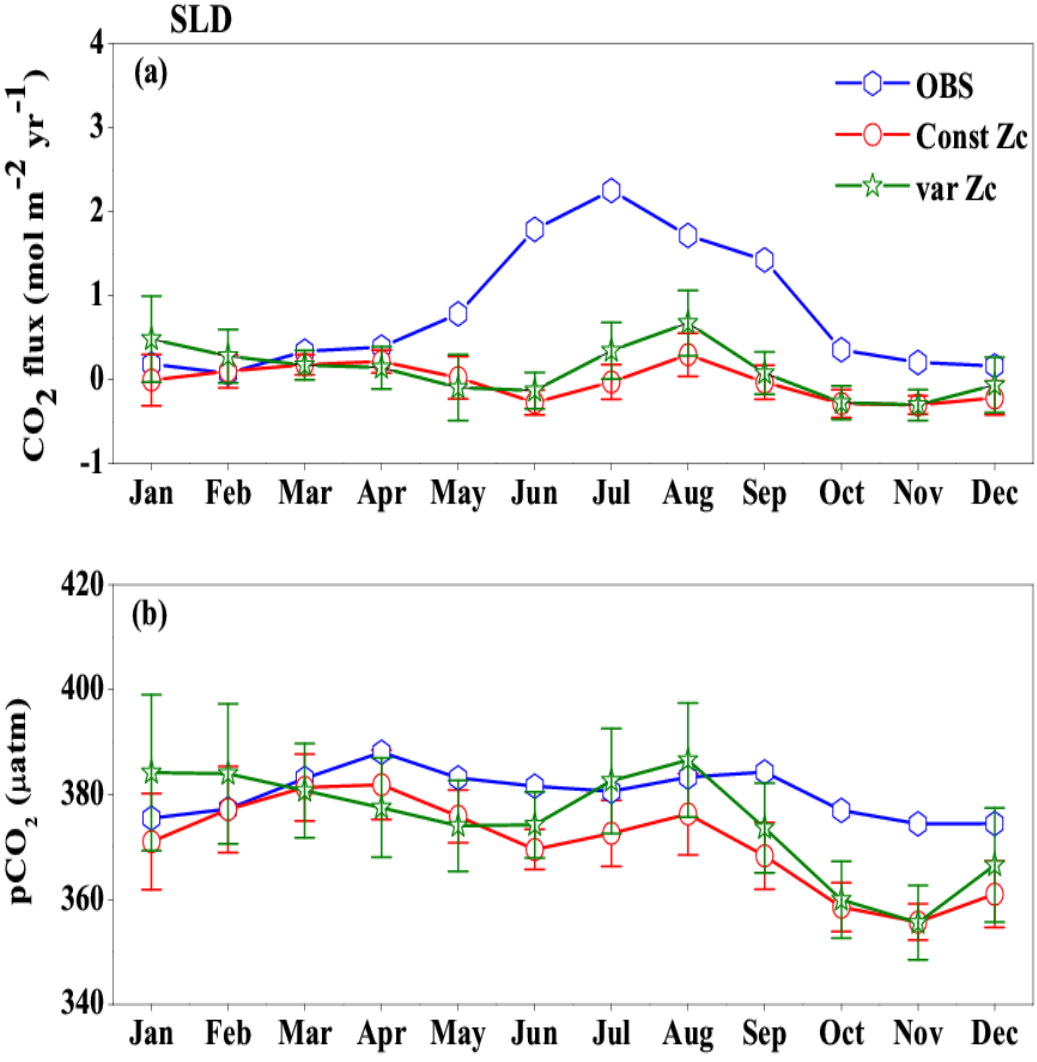

Fig (9): Same as fig (6), but for Srilankan Dome (SLD) region.

Biogeosciences Discuss., doi:10.5194/bg-2017-114, 2017
Manuscript under review for journal Biogeosciences
Discussion started: 28 April 2017

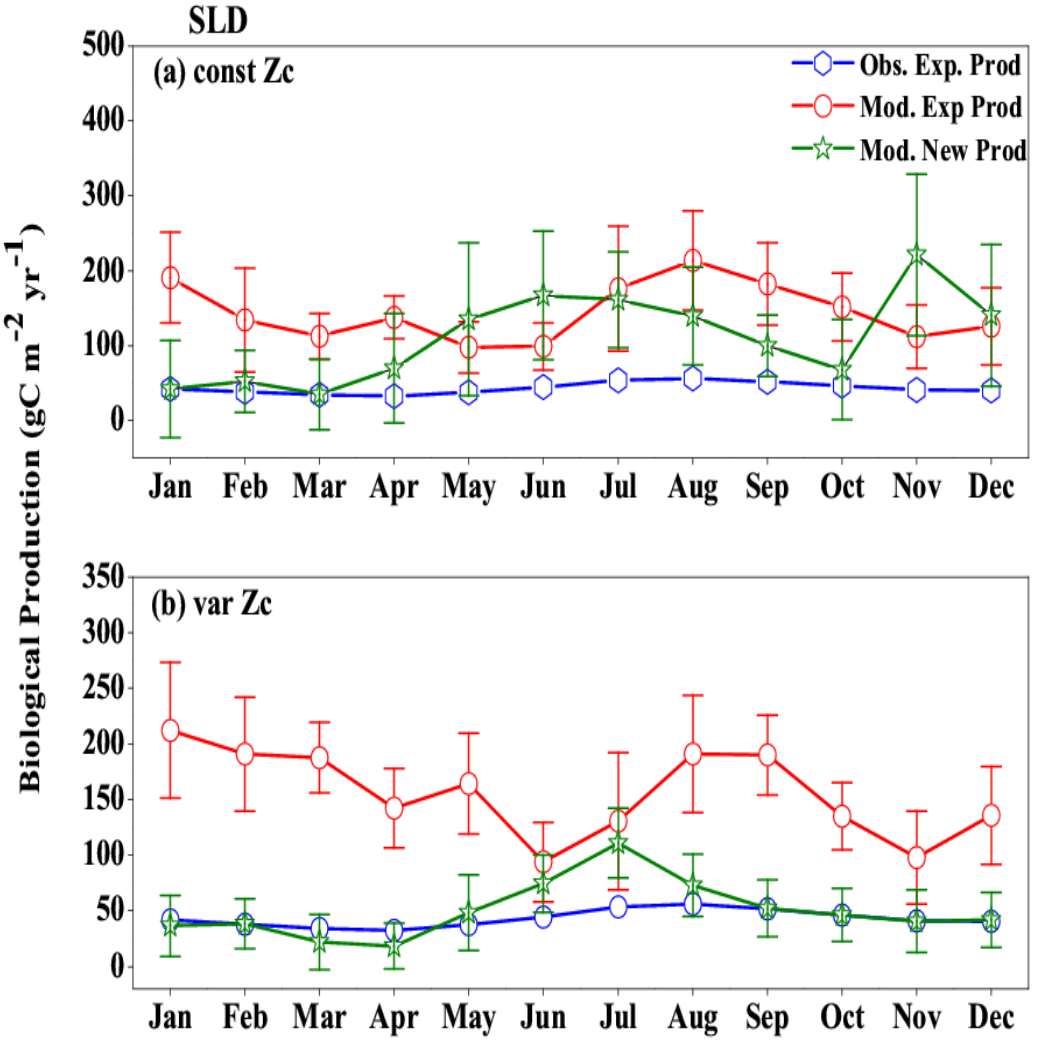

Fig (10): Same as fig (7), but for Srilankan Dome (SLD) region.

Biogeosciences Discuss., doi:10.5194/bg-2017-114, 2017
Manuscript under review for journal Biogeosciences
Discussion started: 28 April 2017

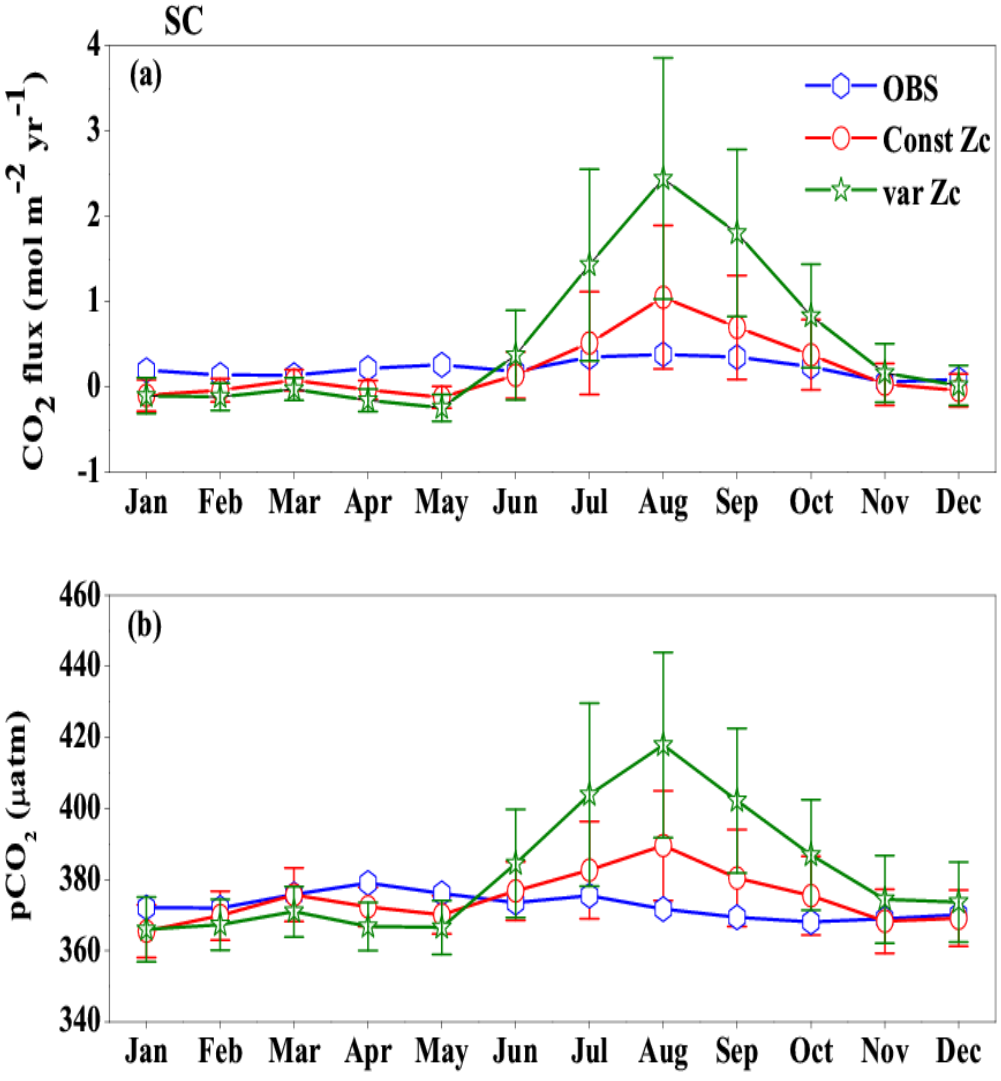

Fig (11): Same as fig (6), but for Sumatra Coast (SC) region.

Biogeosciences Discuss., doi:10.5194/bg-2017-114, 2017
Manuscript under review for journal Biogeosciences
Discussion started: 28 April 2017

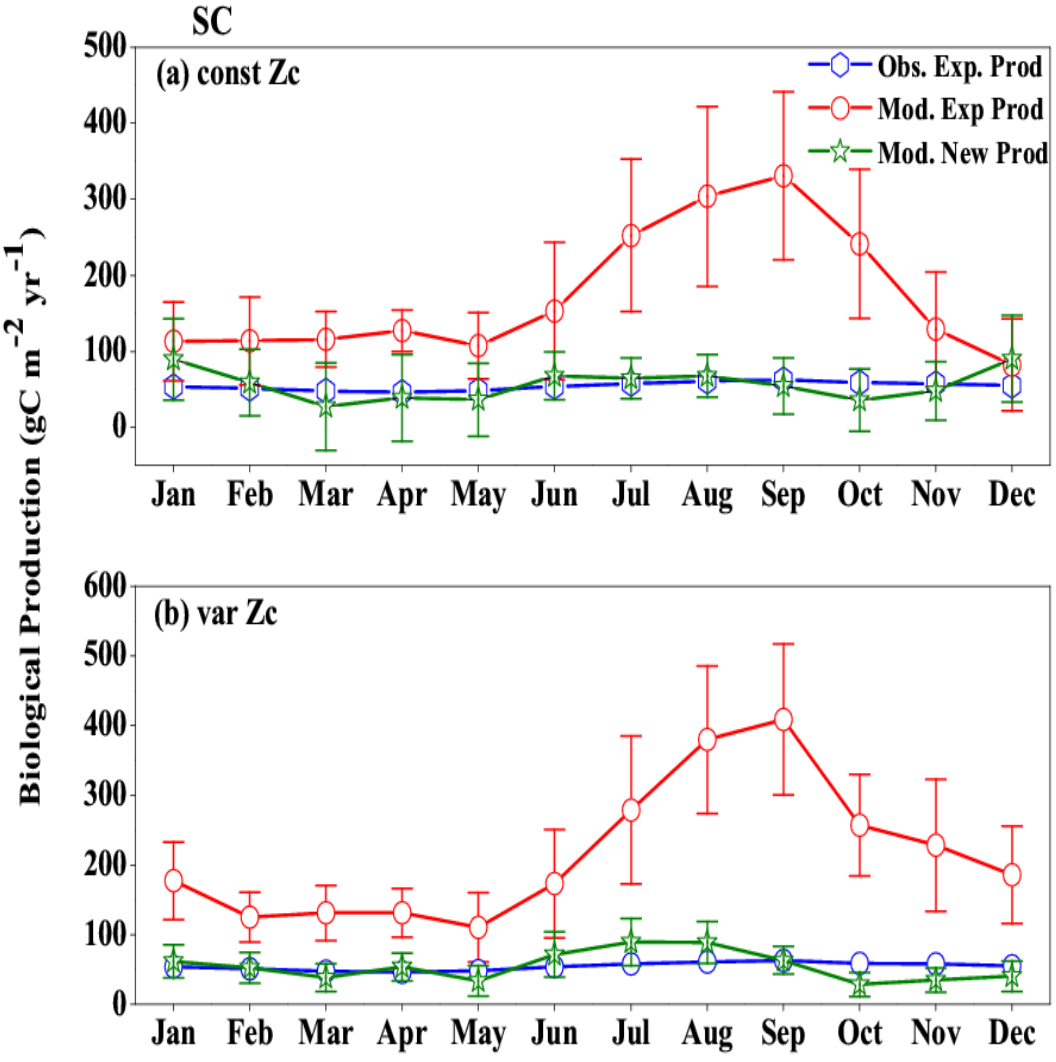

Fig (12): Same as fig (7), but for Sumatra Coast (SC) region.

Biogeosciences Discuss., doi:10.5194/bg-2017-114, 2017
Manuscript under review for journal Biogeosciences
Discussion started: 28 April 2017

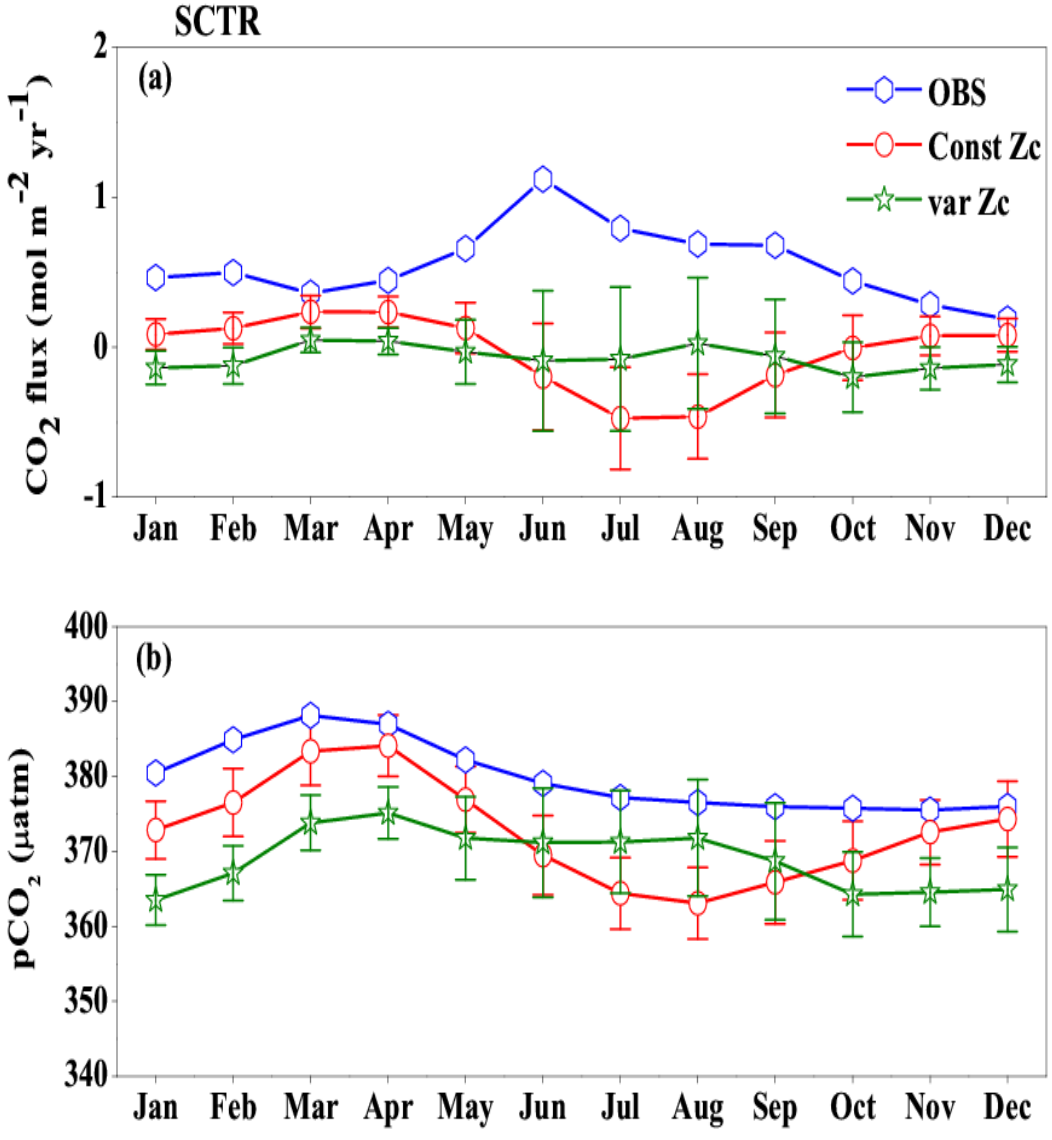

Fig (13): Same as fig (6), but for Seychelles-Chagos Thermocline Ridge (SCTR) region.

Biogeosciences Discuss., doi:10.5194/bg-2017-114, 2017
Manuscript under review for journal Biogeosciences
Discussion started: 28 April 2017

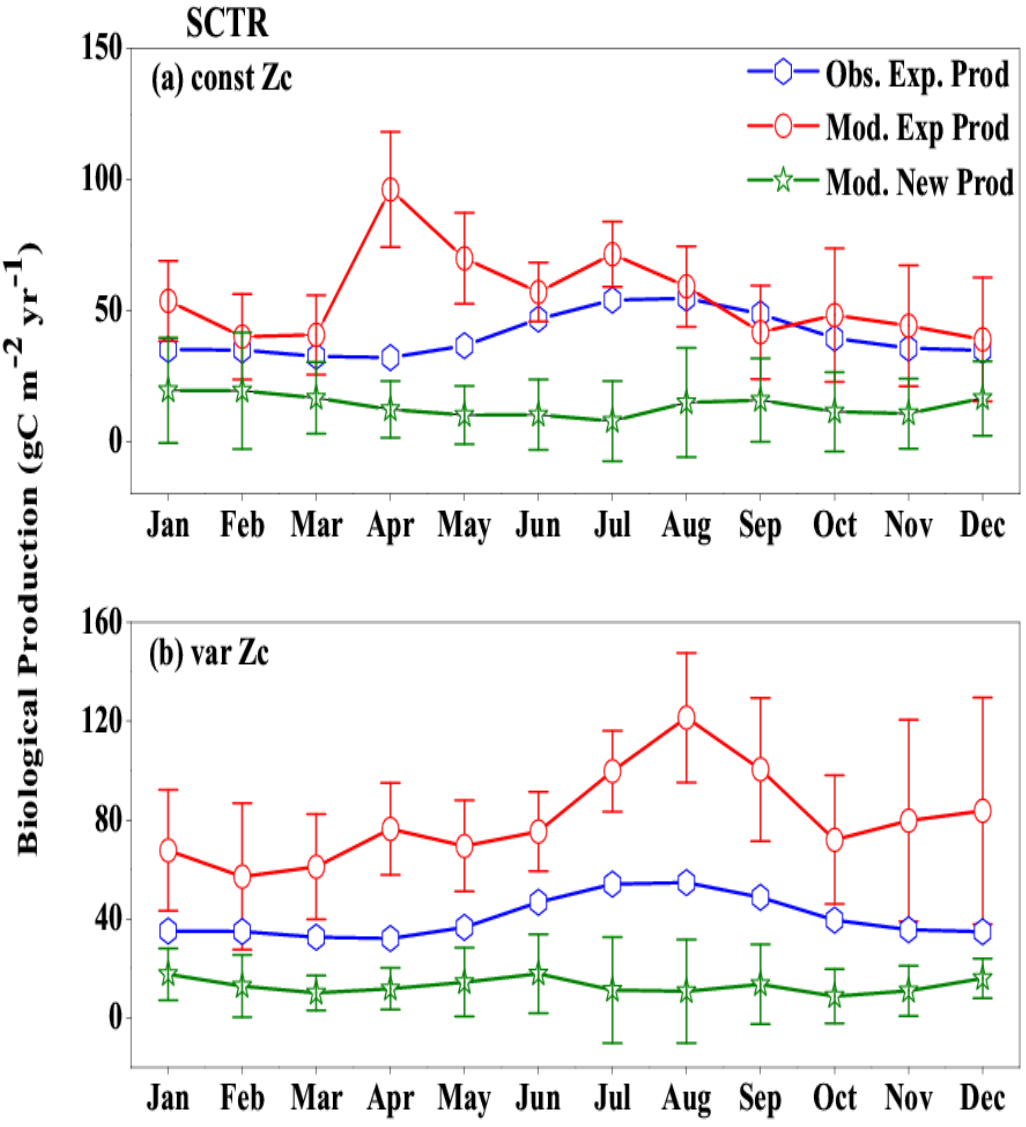

Fig (14): Same as fig (7), but for Seychelles-Chagos Thermocline Ridge (SCTR) region.

Biogeosciences Discuss., doi:10.5194/bg-2017-114, 2017
Manuscript under review for journal Biogeosciences
Discussion started: 28 April 2017

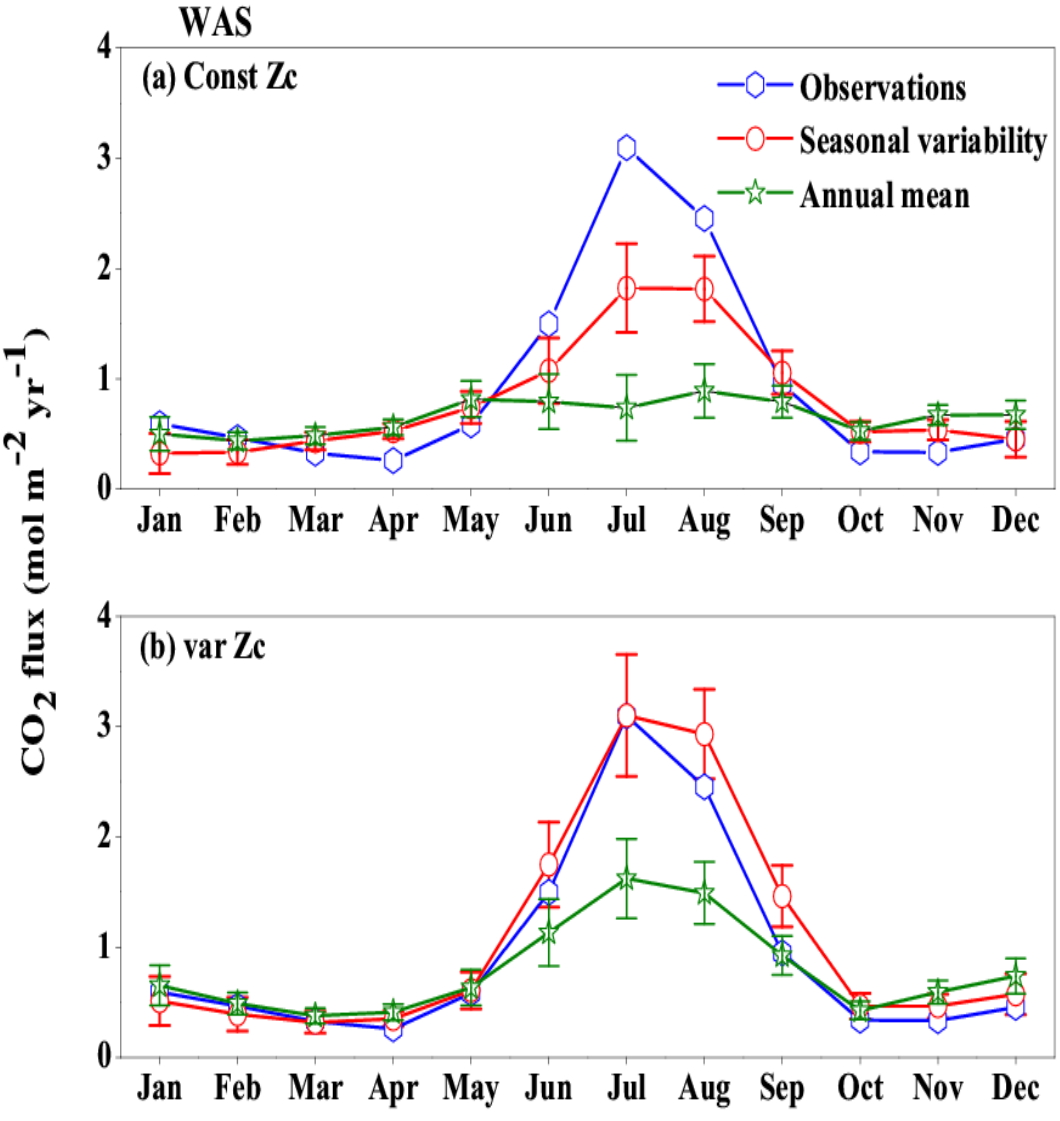

Fig (15) Response of CO_2 flux from the model forced with annual mean currents over the Western Arabian Sea region (WAS) as climatological state computed over 1990-2010. Error bar shows standard deviations of individual months over these years. (a) const Zc and (b) var Zc. Units are in mol m^{-2} yr^{-1}. Legends are same for both graphs.

Biogeosciences Discuss., doi:10.5194/bg-2017-114, 2017
Manuscript under review for journal Biogeosciences
Discussion started: 28 April 2017

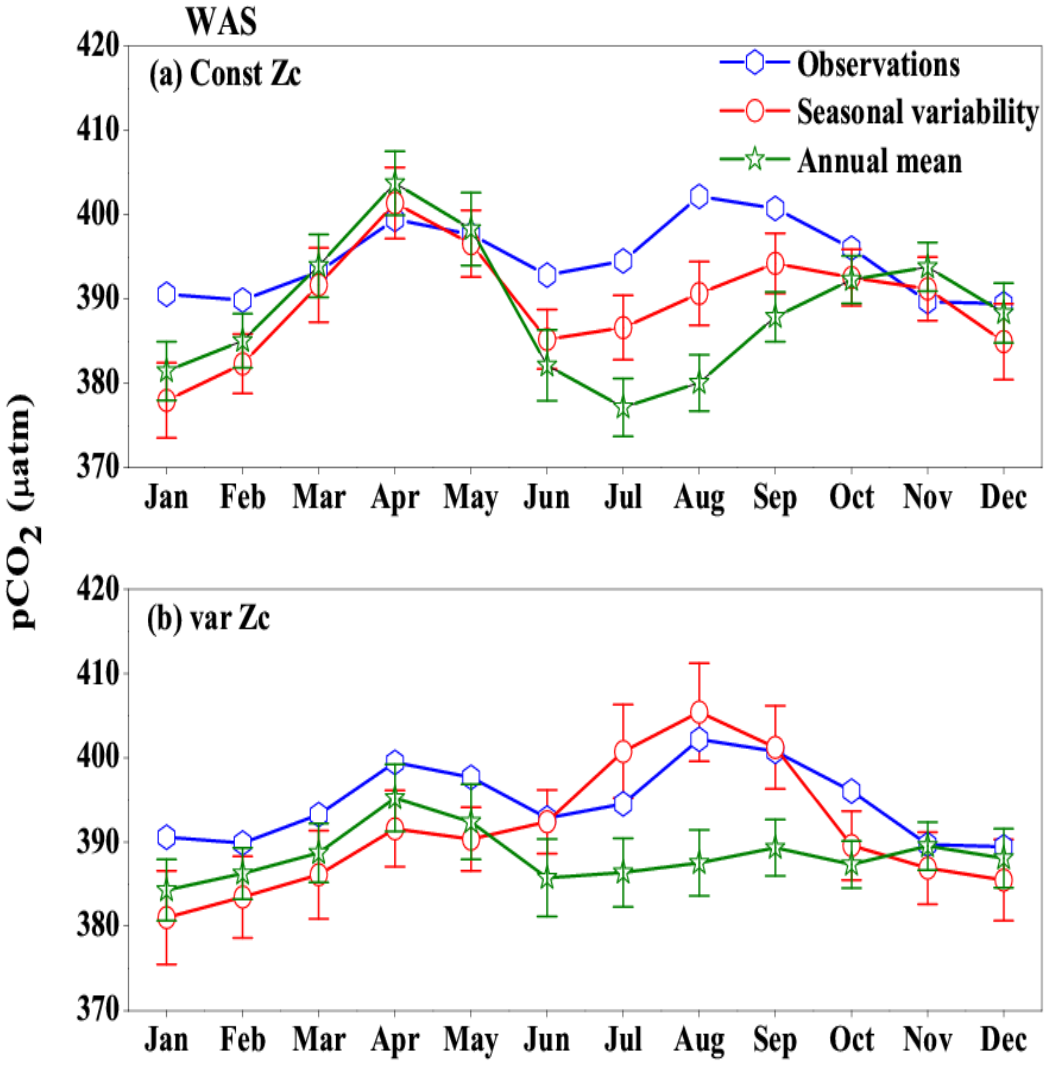

Fig (16) Same as Fig (15), but for pCO_2. Units are in µatm.

Biogeosciences Discuss., doi:10.5194/bg-2017-114, 2017
Manuscript under review for journal Biogeosciences
Discussion started: 28 April 2017

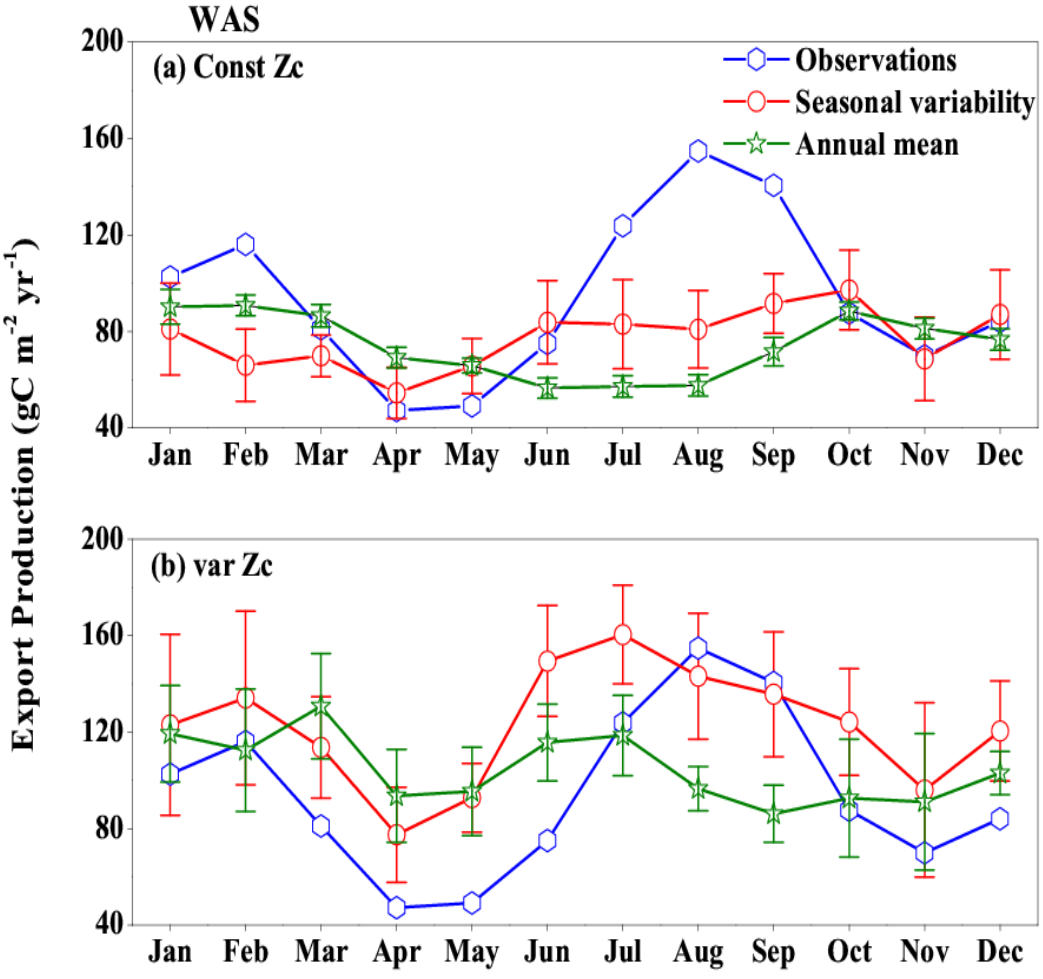

Fig (17) Response in Export Production of the model forced with annual mean currents in the Western Arabian Sea (WAS) region as climatological state computed over 1990-2010. Error bar shows standard deviations of individual months over these years. (a) Const Zc (b) varZc. Units are in g C m^{-2} yr^{-1}. Legends are same for both graphs.

Biogeosciences Discuss., doi:10.5194/bg-2017-114, 2017
Manuscript under review for journal Biogeosciences
Discussion started: 28 April 2017

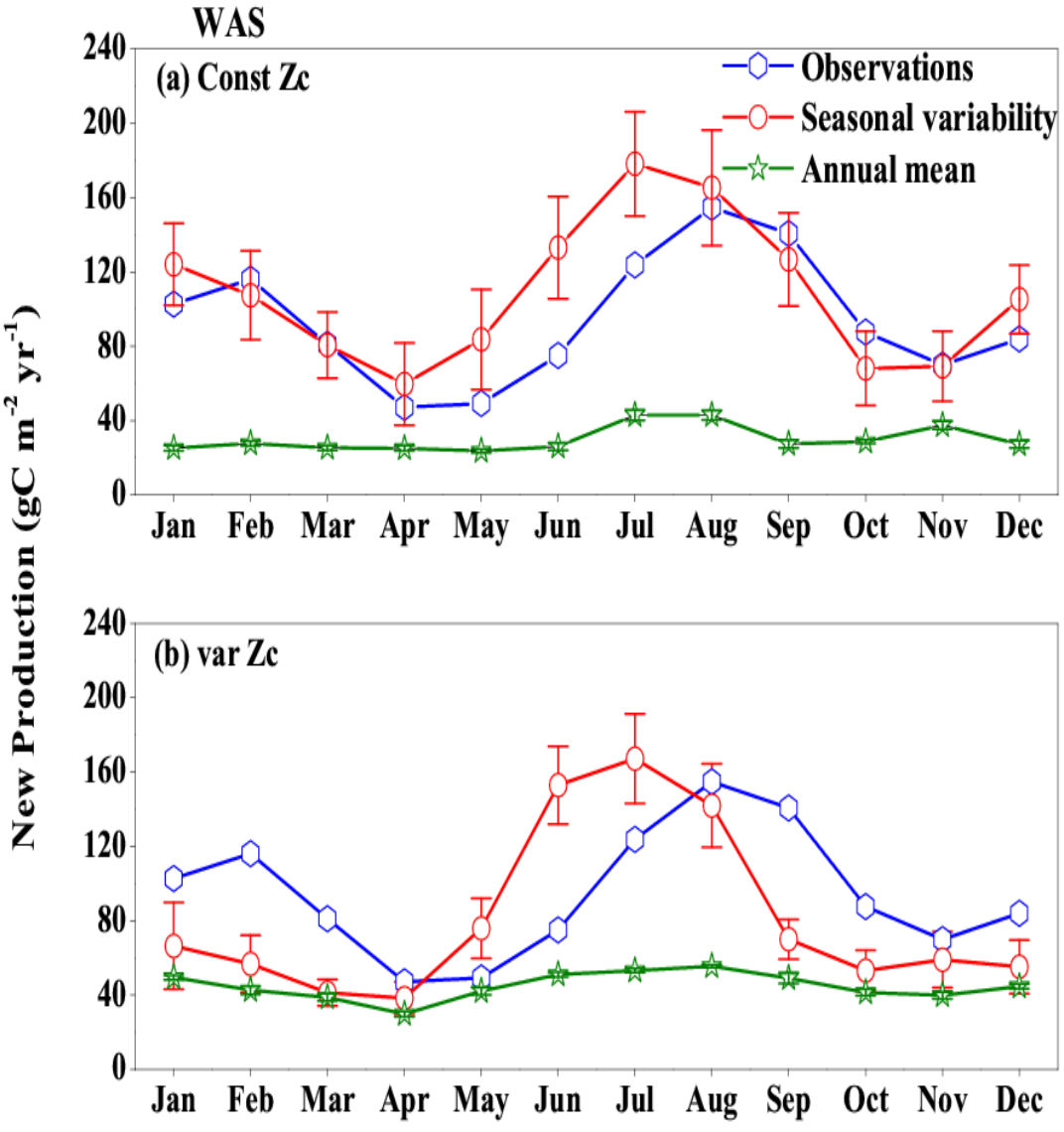

Fig (18) Same as fig (17), but for New Production. Units are in g C m^{-2} yr^{-1}.

Biogeosciences Discuss., doi:10.5194/bg-2017-114, 2017
Manuscript under review for journal Biogeosciences
Discussion started: 28 April 2017

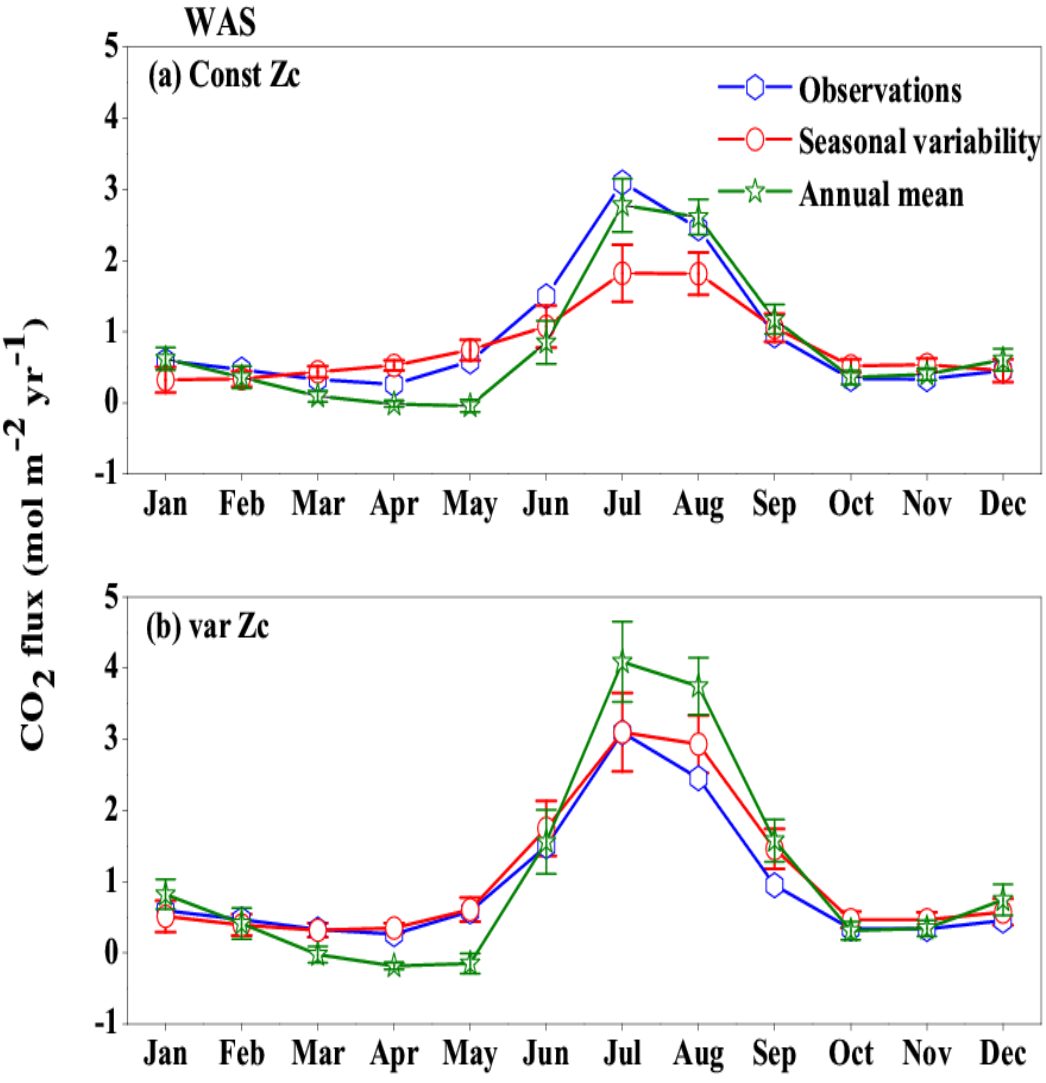

Fig (19) Response of CO_2 flux from the model forced with annual mean SST over the Western Arabian Sea region (WAS) as climatological state computed over 1990-2010. Error bar shows standard deviations of individual months over these years. (a) const Zc and (b) var Zc. Units are in mol m^{-2} yr^{-1}. Legends are same for both graphs.

Biogeosciences Discuss., doi:10.5194/bg-2017-114, 2017
Manuscript under review for journal Biogeosciences
Discussion started: 28 April 2017

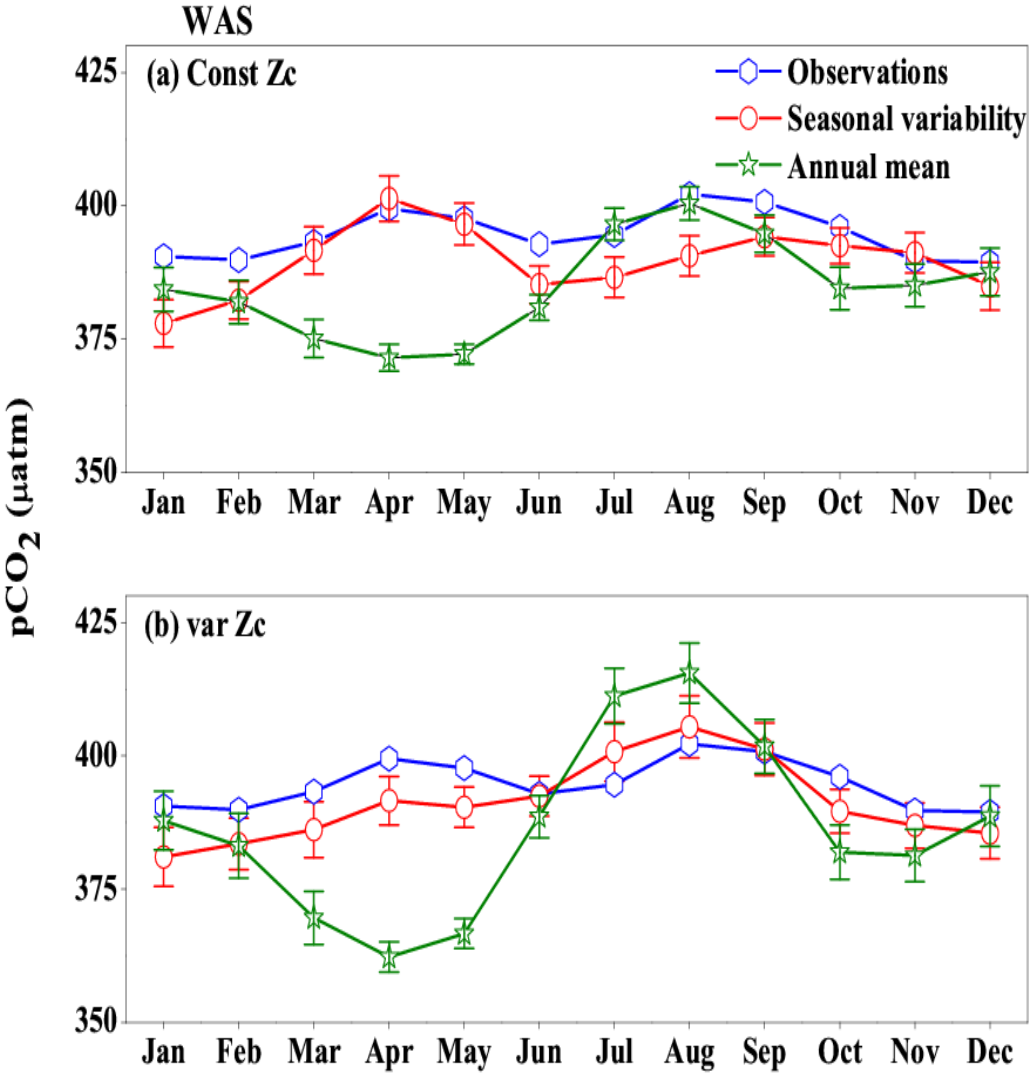

Fig (20). Same as Fig (19), But for pCO_2. Units are in µatm.